

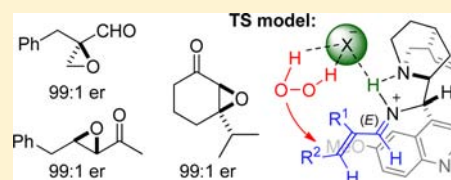
# The Cinchona Primary Amine-Catalyzed Asymmetric Epoxidation and Hydroperoxidation of $\alpha,\beta$ -Unsaturated Carbonyl Compounds with Hydrogen Peroxide

Olga Lifchits, Manuel Mahlau, Corinna M. Reisinger, Anna Lee, Christophe Farès, Iakov Polyak, Gopinadhanpillai Gopakumar, Walter Thiel, and Benjamin List\*

Max-Planck-Institut für Kohlenforschung, Kaiser-Wilhelm-Platz 1 D-45470, Mülheim an der Ruhr, Germany

**S** Supporting Information

**ABSTRACT:** Using cinchona alkaloid-derived primary amines as catalysts and aqueous hydrogen peroxide as the oxidant, we have developed highly enantioselective Weitz–Scheffer-type epoxidation and hydroperoxidation reactions of  $\alpha,\beta$ -unsaturated carbonyl compounds (up to 99.5:0.5 er). In this article, we present our full studies on this family of reactions, employing acyclic enones, 5–15-membered cyclic enones, and  $\alpha$ -branched enals as substrates. In addition to an expanded scope, synthetic applications of the products are presented. We also report detailed mechanistic investigations of the catalytic intermediates, structure–activity relationships of the cinchona amine catalyst, and rationalization of the absolute stereoselectivity by NMR spectroscopic studies and DFT calculations.



## INTRODUCTION

Since the seminal discoveries of Sharpless in the 1980s,<sup>1</sup> catalytic olefin epoxidation has continued to hold a prominent place in modern asymmetric synthesis. Milestone achievements in this field over the last thirty years, including those associated with the names of Juliá and Colonna, Wynberg, Jackson, Jacobsen, Katsuki, Enders, Shi, and Shibasaki, have not only provided reliable synthetic protocols but also identified entirely novel catalytic platforms.<sup>2</sup>

One of the most fundamental ways to form an oxirane ring is the reaction of basic hydrogen peroxide with electrophilic  $\alpha,\beta$ -unsaturated ketones and aldehydes, a process described already in 1921 by Weitz and Scheffer.<sup>3</sup> Kinetic studies of this transformation established it to be a two-step addition–elimination process, in which hydrogen (or alkyl) peroxide, deprotonated under basic conditions, adds to the  $\beta$ -carbon of the unsaturated carbonyl compound, forming a  $\beta$ -peroxyenolate intermediate **B** (Scheme 1a).<sup>4</sup> This is followed by an intramolecular ring closure, in which the weak O–O bond is broken and a second C–O bond is formed, expelling a hydroxide or an alkoxide anion as the leaving group. Protonation of the enolate **B** results in the common side-product of the reaction, hydroperoxide **D** (typically observed in its more stable hemiketal form as shown). Several enantioselective variants of the Weitz–Scheffer epoxidation have been developed to date, which rely on the catalytic activation of the substrate and/or the peroxide reagent. Most recently, it has been recognized that Weitz–Scheffer-type epoxidation is also amenable to covalent aminocatalysis, whereby the carbonyl substrates are activated as iminium ion intermediates **E** toward conjugate addition by the oxidant (Scheme 1b).

The resulting peroxyenamine **F** then undergoes epoxide ring closure with the expulsion of water, much like in the original Weitz–Scheffer system.

This catalytic platform proved to be highly efficient for the epoxidation of unencumbered  $\alpha$ -unbranched  $\alpha,\beta$ -unsaturated aldehydes, as demonstrated by the seminal works of Jørgensen and later MacMillan who used various chiral secondary amines as catalysts.<sup>5</sup> Our group has also contributed to this reaction in 2008 with the use of asymmetric counteranion-directed catalysis (ACDC), in which an achiral secondary amine catalyst together with the chiral Brønsted acid TRIP were used to induce enantioselectivity.<sup>6</sup>

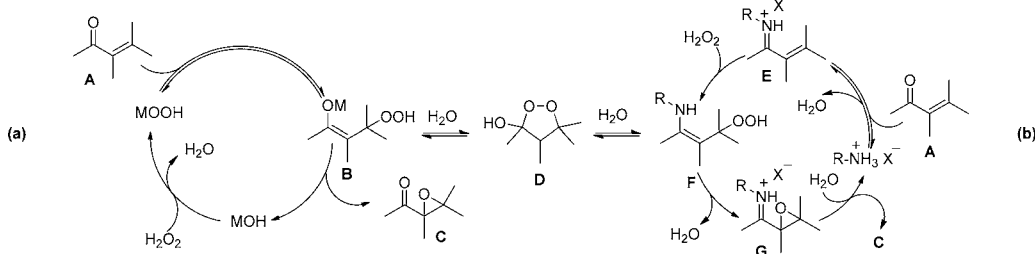
Despite the success of secondary amine catalysts in the epoxidation of  $\alpha$ -unbranched enals, their extension to more sterically demanding substrates remained a challenge.<sup>7</sup> Furthermore, at the outset of our studies, the enantioselective epoxidation of simple cyclic enones, nonchalcone-type acyclic enones, and  $\alpha$ -branched enals presented a general problem, for which neither metal- nor small organic molecule-based catalysis offered highly enantioselective protocols.

Our early interest in the use of primary amine catalysts as a tool to tackle difficult substrates prompted us to explore this catalyst class in various transformations.<sup>8</sup> For example, in 2006 we developed a highly enantioselective transfer hydrogenation of enones using an  $\alpha$ -amino acid ester/chiral phosphate salt.<sup>8a</sup> Encouraged by this and other seminal studies,<sup>9</sup> we sought to apply primary amine catalysis to asymmetric epoxidation of challenging  $\alpha,\beta$ -unsaturated carbonyl compounds. As a guiding principle, we relied on the assumption that the reduced steric requirements of primary amines may overcome the inherent

Received: March 5, 2013

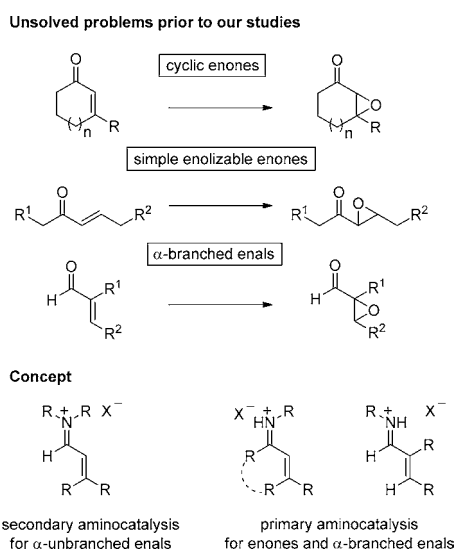
Published: April 18, 2013

Scheme 1. Weitz-Scheffer Epoxidation: (a) the Original Mechanism and (b) the Amine-Catalyzed Variant



difficulties of secondary amines in generating congested covalent iminium ion intermediates (Scheme 2).<sup>10</sup>

Scheme 2. Challenging Substrate Classes Prior to our Studies and our Proposed Catalytic Platform



Thus, we speculated that if primary amine salts are compatible with oxidizing conditions, they could provide a general solution for the epoxidation of sterically demanding substrates. Indeed, both iminium and enamine catalysis employing chiral primary amines have started to emerge as a powerful strategy in catalytic asymmetric transformations in recent years.<sup>2e,10,11</sup> Initial investigations using the salts of cinchona alkaloid-derived primary amine catalyst **1a**<sup>11a-c,g,12</sup> confirmed our expectations, and we have recently developed and communicated highly enantioselective epoxidation and hydroperoxidation reactions of a variety of cyclic and acyclic enones as well as  $\alpha$ -branched enals.<sup>8b,c,e</sup> Subsequent to our initial report,<sup>8c</sup> Deng et al. independently published related alkylperoxidations of acyclic enones using catalyst **1a**.<sup>11e</sup>

All of the reactions employ catalyst **1a** or its close analogues and feature both generality and a remarkable consistency in the stereochemical outcome. Herein, we present our full studies on this family of reactions, including an expansion of the scope, synthetic applications, and mechanistic investigations.

## RESULTS AND DISCUSSION

**Epoxidation and Hydroperoxidation of Acyclic Enones.**<sup>8b</sup> At the outset of our studies in 2008, general and highly enantioselective strategies for the catalytic epoxidation of simple,  $\alpha,\beta$ -unsaturated ketones were scarce.<sup>2j,13</sup> Indeed, despite the wealth of epoxidation methodologies, only

chalcone-type substrates were broadly suitable, with simple enolizable aliphatic enones still posing a considerable challenge to chemists.<sup>2b,d,g,l,14</sup>

Inspired by our earlier success with primary amine catalysis,<sup>8a</sup> we decided to examine trifluoroacetic acid (TFA) salts of the cinchona alkaloid-derived amine **1a** in this transformation. Using 3-decen-2-one (**2a**) as a model substrate and hydrogen peroxide as an inexpensive, environmentally benign, and easily handled oxidant, we observed complete conversion of the starting material to two isolable products: cyclic peroxyhemiketal **3a**, a known intermediate and common byproduct in Weitz-Scheffer-type epoxidations,<sup>15</sup> and the expected epoxide **4a** as the minor product in essentially enantiopure form.

Since cyclic peroxides **3** can be quantitatively transformed into the corresponding epoxides **4** under basic conditions,<sup>16</sup> and serve as precursors to other useful compounds, we decided to first optimize the hydroperoxidation reaction. The ratio of the intermediate peroxyhemiketal **3** and the terminal epoxide product **4** was found to mainly depend on the  $pK_a$  of the acid cocatalyst, water content, and temperature of the reaction, with weaker acids, higher water concentration, and lower reaction temperature favoring the hydroperoxidation product and decelerating the formation of the epoxidation product.<sup>17</sup> With the optimal conditions in hand, we evaluated the scope of the reaction, employing various aliphatic enones **2** (Table 1). A wide variety of substrates was found to be compatible with the reaction, affording the desired cyclic peroxyhemiketals **3** as the major products, which could be easily separated from the epoxide side-products **4** and isolated with reasonable yields and invariably excellent enantioselectivities. Both linear and branched aliphatic substituents  $R^1$  were well tolerated (entries 1–4), although the degree of branching affected the hydroperoxide/epoxide product distribution. Functional groups including an isolated double bond (entry 5), acid-labile protected alcohol moieties (entries 6–7), an ester (entry 8), a pendant ketone (entry 9), and an unprotected hydroxy group (entry 10) were acceptable. Notably, the second ketone group in substrate **2j** gave rise to an equilibrium mixture of two cyclic peroxyhemiketal products, containing five- and six-membered dioxolane rings.<sup>17</sup> Five-membered peroxyhemiketal **3j'** was found to exist as the typical mixture of two diastereomers, while only one diastereomer of the six-membered isomer **3j''** could be detected, whose relative configuration was putatively assigned.

Various groups  $R^2$ , which render substrates **2** enolizable, all participated in the reaction smoothly (entries 13–17), although higher steric demand of the  $R^2$  group was found to decrease reactivity and increasingly favor the formation of the epoxide products **4**. Surprisingly, substrate **2m** bearing an isobutyl group almost exclusively afforded the epoxide product (entry 14).

Table 1. Catalytic Asymmetric Hydroperoxidation of Enones

entry <sup>a</sup>	R <sup>1</sup>	R <sup>2</sup>	product	3:4 ratio <sup>b</sup>	yield (3) [%]	er (3) <sup>c</sup>
1 <sup>d</sup>	<i>n</i> -C <sub>6</sub> H <sub>13</sub>	Me	<b>3a</b>	80:20	65	98.5:1.5
2	PhCH <sub>2</sub> CH <sub>2</sub>	Me	<b>3b</b>	78:22	68	97:3
3	<i>i</i> -Bu	Me	<b>3c</b>	71:29	61	97.5:2.5
4	Cy	Me	<b>3d</b>	68:32	54	98:2
5		Me	<b>3e</b>	80:20	69	97.5:2.5
6		Me	<b>3f</b>	79:21	72	97:3
7		Me	<b>3g</b>	76:24	64	96.5:3.5
8		Me	<b>3h</b>	80:20	68	98:2
9		Me	<b>3i</b>	85:15	70	96.5:3.5
10		Me	<b>3j</b>	63:37	30	96:4
11		Me	<b>3k</b>	-	25 <sup>e</sup>	(98:2) <sup>f</sup>
13	<i>n</i> -C <sub>5</sub> H <sub>11</sub>	<i>n</i> -C <sub>5</sub> H <sub>11</sub>	<b>3l</b>	45:55	40	97:3
14	<i>n</i> -C <sub>5</sub> H <sub>11</sub>	<i>i</i> -Bu	<b>3m</b>	5:95	-	-
15	Me	<i>i</i> -Pr	<b>3n</b>	50:50	39 <sup>g</sup>	96:4
16	Me	Et	<b>3o</b>	74:26	56	97:3
17	<i>n</i> -C <sub>9</sub> H <sub>19</sub>	Et	<b>3p</b>	63:37	48	98:2

<sup>a</sup>All reactions performed on 0.5–1 mmol scale. <sup>b</sup>Determined by <sup>1</sup>H NMR analysis of the crude reaction mixture. <sup>c</sup>Determined by GC with a chiral stationary phase after conversion to the corresponding epoxide with 1 N NaOH (1 equiv) in THF. <sup>d</sup>Conducted on 3 mmol scale. <sup>e</sup>69% conversion determined by <sup>1</sup>H NMR. <sup>f</sup>er of the initially formed epoxide **4k**. <sup>g</sup>96% conversion determined by <sup>1</sup>H NMR.

A slight modification of the reaction conditions and an inclusion of a basic workup of the crude reaction mixture with 1N NaOH allowed for an efficient generation of epoxide products **4** (Table 2).

Gratifyingly, good to excellent yields and very good enantioselectivities were obtained for a range of substrates of varying steric demands. Importantly, using the pseudoenantiomeric catalyst **1b**, the opposite enantiomers of the epoxide products could be accessed with nearly equal efficiency (entries 1–2 and 3–4). Interestingly, both substrates **2r** bearing a bulky R<sup>1</sup> group (entry 7) and **2m** bearing a bulky R<sup>2</sup> group (entry 21) afforded the respective epoxide products with essentially perfect enantiocontrol (er >99.5:0.5). In addition, epoxide **4m** (entry 21) was formed as the only product of the reaction, whereby no corresponding peroxyhemiketal product could be detected. All of the functional groups which were found to be compatible in the hydroperoxidation procedure (Table 1) were also suitable for epoxidation (entries 10–16). However, the hydrolyzing conditions of aqueous NaOH workup required in the epoxidation protocol resulted in partial saponification of

Table 2. Catalytic Asymmetric Epoxidation of Enones

entry <sup>a</sup>	R <sup>1</sup>	R <sup>2</sup>	product	yield, [%]	er <sup>c</sup>
1	<i>n</i> -C <sub>6</sub> H <sub>13</sub>	Me	<b>4a</b>	75	98.5:1.5
2 <sup>d</sup>	<i>n</i> -C <sub>6</sub> H <sub>13</sub>	Me	<b>ent-4a</b>	81	96:4
3	PhCH <sub>2</sub> CH <sub>2</sub>	Me	<b>4b</b>	85	98.5:1.5
4 <sup>d,e</sup>	PhCH <sub>2</sub> CH <sub>2</sub>	Me	<b>ent-4b</b>	90	95:5
5	PhCH <sub>2</sub>	Me	<b>4q</b>	70 <sup>b,c</sup>	99:1
6	<i>i</i> -Bu	Me	<b>4c</b>	77	98.5:1.5
7	<i>t</i> BuCH <sub>2</sub>	Me	<b>4r</b>	81	>99.5:0.5
8	<i>i</i> -Pr	Me	<b>4s</b>	50 <sup>f</sup>	98:2
9	Cy	Me	<b>4d</b>	84	98.5:1.5
10		Me	<b>4e</b>	76	98.5:1.5
11		Me	<b>4f</b>	75	98.5:1.5
13		Me	<b>4g</b>	88	98:2
14		Me	<b>4h</b>	72	98.5:1.5
15 <sup>g</sup>		Me	<b>4i</b>	81	98:2
16 <sup>h</sup>		Me	<b>4j</b>	40	98.5:1.5
17		Me	<b>4k</b>	51 <sup>i</sup>	98:2
18	Me	Et	<b>4o</b>	55 <sup>g</sup>	98.5:1.5
19	<i>n</i> -C <sub>9</sub> H <sub>19</sub>	Et	<b>4p</b>	82	99:1
20	<i>n</i> -C <sub>5</sub> H <sub>11</sub>	<i>n</i> -C <sub>5</sub> H <sub>11</sub>	<b>4l</b>	76	99:1
21 <sup>j,h</sup>	<i>n</i> -C <sub>5</sub> H <sub>11</sub>	<i>i</i> -Bu	<b>4m</b>	81	>99.5:0.5
22 <sup>j</sup>	Me	<i>i</i> -Pr	<b>4n</b>	60 <sup>f</sup>	96.5:3.5

<sup>a</sup>All reactions performed on 0.5–1 mmol scale. <sup>b</sup>Determined by <sup>1</sup>H NMR analysis of the crude reaction mixture. <sup>c</sup>Determined by GC with a chiral stationary phase. <sup>d</sup>Using 10 mol % [**1b**-2TFA]. <sup>e</sup>Sum of **3q** and the corresponding peroxyhemiketal **4q** at 94% conversion determined by <sup>1</sup>H NMR. <sup>f</sup>Reduced yield due to the volatility of the product. <sup>g</sup>NaOEt (1 equiv) was used instead of NaOH. <sup>h</sup>Second step was omitted. <sup>i</sup>Sum of **4k** and the corresponding peroxyhemiketal **3k** at 69% conversion determined by <sup>1</sup>H NMR. <sup>j</sup>Using 20 mol % [**1a**-2TFA].

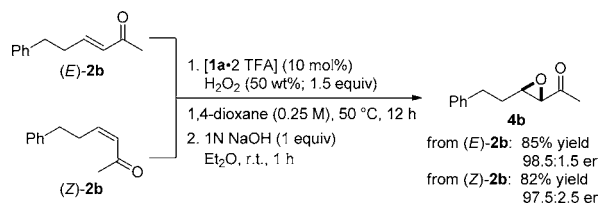
product **4i** (entry 15) which bears an ethyl ester group. This problem could be overcome by using NaOEt in ethanol instead of aqueous NaOH in the workup. In case of the ketone-bearing substrate **2j** (entry 16) the basic workup was omitted since it did not improve the yield of epoxide **4j**, presumably due to a competing base-catalyzed aldol reaction. Thus, epoxide **4j** was isolated from the hydroperoxide–epoxide product mixture in 40% yield and 98.5:1.5 er (entry 16). Low conversion (69%) of 9-hydroxy-3-nonen-2-one **2k** containing an unprotected hydroxyl group, which could not be improved by an extended reaction time, resulted in only moderate yield of the corresponding products, although the enantioselectivity remained high (98:2 er, entry 17).<sup>18</sup>

We also investigated the influence of olefin geometry on the enantioselectivity of the epoxidation reaction by submitting



isomerically pure enones (*E*)-**2b** and (*Z*)-**2b** to the optimal reaction conditions (Scheme 3). Remarkably, both substrates

### Scheme 3. Stereoconvergence in the Asymmetric Epoxidation

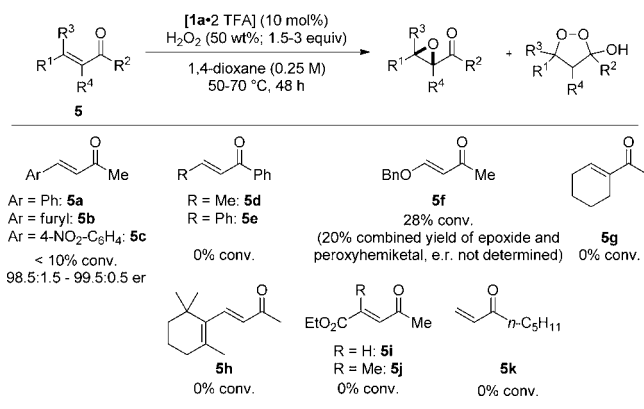


furnished the same enantiomer of *trans*-epoxide **4b** with excellent enantioselectivity and yield, indicating complete stereoconvergence. This behavior suggests that *E/Z* mixtures of enones can be conveniently employed as epoxidation substrates.

GC-MS analysis of samples taken from the epoxidation of pure (*Z*)-**2b** revealed the formation of (*E*)-**2b**, indicating rapid isomerization of the (*Z*)-enone to the corresponding (*E*)-isomer under the reaction conditions. (*Z*)-**2b** was also found to isomerize in the presence of catalytic salt [1a·2 TFA] alone, without any assistance of hydrogen peroxide. This suggests that isomerization may take place via a dienamine intermediate, which allows free rotation about the carbon–carbon single bond. We, and others, have proposed an analogous mechanism in earlier studies on the asymmetric transfer hydrogenation of  $\alpha,\beta$ -unsaturated aldehydes with a secondary amine catalyst, where similar stereoconvergence was observed.<sup>19,20</sup>

Several substrate classes currently represent a limitation of the method and are summarized in Scheme 4. Enones

### Scheme 4. Current Limitations in Enone Hydroperoxidation and Epoxidation



conjugated with an aromatic group (**5a–c**, **5e**) all gave the corresponding epoxide products in <10% yield, albeit with high enantioselectivity of 98.5:1.5–99.5:0.5 er. Considerable amount (up to 12%) of the starting material **5a** was found to decompose to phenylacetaldehyde, presumably via a Dakin-type reaction.<sup>21</sup> The use of electron-poorer and thus more activated Michael acceptors, such as **5c**, suppressed this side reaction but did not improve the yield. Other aromatic enones, such as furfurylideneacetone (**5b**), 1-phenyl-2-buten-1-one (**5d**), and chalcone (**5e**), proved to be unreactive under the reaction conditions.

Thus, both substituents  $R^1$  and  $R^2$  are limited to alkyl groups, a phenomenon also observed by Deng and colleagues in the 1a-catalyzed hydroperoxidation of  $\alpha,\beta$ -unsaturated ketones with *tert*-butyl peroxide and related oxidants.<sup>11c</sup> Similarly, literature analysis confirmed that the aromatic  $R^2$  substituents (Scheme 4) are only very rarely tolerated in reactions catalyzed by cinchona alkaloid-derived primary amines.<sup>22</sup> In this respect, our catalytic epoxidation complements conventional methods, such as metal-catalyzed or Juliá-Colonna epoxidations.

Despite the reaction's tolerance of remote protected hydroxy functionalities, a benzyloxy group in the  $\gamma$  position proved deleterious (substrate **5f**). Neither substitution at the  $\alpha$ -position nor extended conjugation of the double bond is tolerated, as illustrated by the reaction of 1-acetylcyclohexene (**5g**) and  $\beta$ -ionone (**5h**), respectively. 4-Oxoenoates **5i–j** also did not undergo epoxidation, although their use in related transformations via asymmetric iminium ion catalysis is well precedented in the literature. Surprisingly, terminal enones were unsuitable in the reaction (substrate **5k**). We speculate that in the case of more active Michael acceptors, conjugate addition of catalyst **1a** to form  $\beta$ -amino ketones is favored over condensation with the ketone group, especially given that hydrogen peroxide (presumably in its neutral form) is a weak nucleophile to compete with. To probe this hypothesis, we conducted the epoxidation of our model substrate 3-decen-2-one (**2a**) in the presence of the terminal enone **5k** (1:1 ratio), adjusting the reaction parameters to imitate the optimal conditions. Only epoxide **4a** was generated, albeit at a significantly lower rate. This is consistent with the assumption that the catalyst is captured as a  $\beta$ -amino ketone by **5k** and only partly released from this “catalyst resting state”, keeping its absolute concentration low.<sup>23</sup>

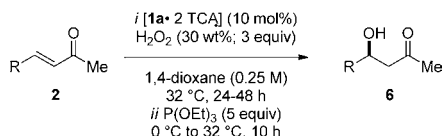
**Synthetic Utility of the Obtained Epoxides and Hydroperoxides.** To demonstrate the utility of our hydroperoxidation and epoxidation reactions, we also explored several synthetic applications of the corresponding products **3** and **4**.

We recognized that a simple reduction of the O–O bond in hydroperoxides **3** could deliver valuable  $\beta$ -hydroxyketones **6**. Importantly, organocatalytic aldol approaches to these compounds are limited by the need to use unbranched enolizable aldehydes, which are prone to self-aldolization and typically lead to lower yields and inferior enantioselectivities. In contrast, hydroperoxidation of enones **2** followed by reduction, which represents a formal enantioselective hydration of the  $\alpha,\beta$ -unsaturated ketones, could furnish  $\beta$ -hydroxyketones **6** from simple starting materials and draw upon the high enantioselectivity of our hydroperoxidation procedure.

Based on this rationale, we developed a one-pot protocol which consists of asymmetric hydroperoxidation, followed by the addition of triethylphosphite<sup>24</sup> to the crude reaction mixture. Various aldol-like products **6** were thus obtained in good yields and excellent enantioselectivities (Table 3).

Alternatively, the crude peroxyhemiketals can also be reduced by catalytic hydrogenation with equal efficiency and without any erosion of the enantiomeric excess (Table 3, entry 2).<sup>26</sup>

The existence of potent natural products which contain optically active five-membered 1,2-dioxolanes<sup>27</sup> and the noticeable lack of methodologies for their asymmetric synthesis in the chemical literature<sup>28</sup> stimulated us to seek approaches to this substrate class based on our methodology. We envisaged optically active peroxyhemiketals **3** as precursors for the

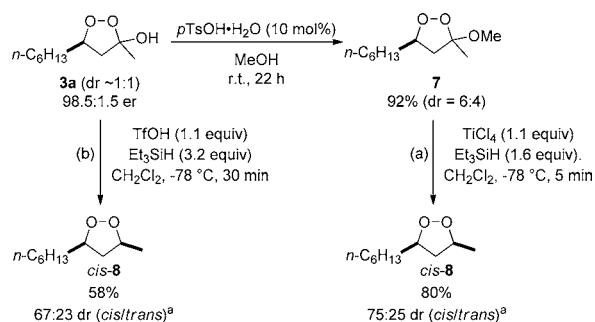
Table 3. One-Pot Synthesis of  $\beta$ -Hydroxyketones

entry	R	product	yield (6), [%]	er (6) <sup>a</sup>
1	<i>n</i> -C <sub>6</sub> H <sub>13</sub>	<b>6a</b>	59	97:3
2 <sup>b</sup>	<i>n</i> -C <sub>6</sub> H <sub>13</sub>	<b>6a</b>	61	97:3
3	PhCH <sub>2</sub> CH <sub>2</sub>	<b>6b<sup>c</sup></b>	53	96.5:3.5
4	<i>i</i> -Bu	<b>6c</b>	56	96.5:3.5
5	Cy	<b>6d</b>	46	96:4
6		<b>6e</b>	55	96:4

<sup>a</sup>Determined by GC or HPLC with a chiral stationary phase. <sup>b</sup>*ii* = H<sub>2</sub> (1 atm), Pd/C (15 wt %), MeOH. <sup>c</sup>Absolute configuration (R) was determined by comparison with literature known optical rotation data.<sup>25</sup>

corresponding 1,2-dioxolanes **8**. Toward this end, we found that simple ketalization of **3a** with methanol and catalytic Brønsted acid followed by triethylsilane reduction in the presence of titanium tetrachloride could afford 1,2-dioxolane **8** in 74% overall yield and a 75:25 diastereomeric ratio in favor of the *cis*-isomer (Scheme 5a). Moreover, dioxolane **8** could be

Scheme 5. Synthesis of 1,2-Dioxolanes



directly obtained in good yield and only slightly lower diastereoselectivity (67:23 dr) via reduction of peroxyhemiketal **3a** with triethylsilane in the presence of stoichiometric amounts of triflic acid, which presumably generates Lewis acidic triethylsilyl triflate under the reaction conditions (Scheme 5b). To the best of our knowledge, this is the first report on the direct conversion of peroxyhemiketals into the corresponding dioxolanes, which obviates the need to preform a peroxyketal.

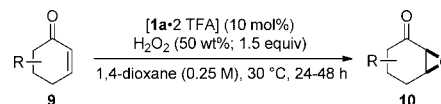
Adapting the conditions of Yamaguchi and colleagues,<sup>29</sup> we could also carry out diastereoselective ketone reduction of epoxides **4** to form optically active epoxyalcohols.<sup>30</sup>

#### Epoxidation of Cyclic Enones: Cyclohexenones.<sup>8c</sup>

Simple cyclic enones have generally been omitted within the vast majority of studies on the asymmetric epoxidation of  $\alpha,\beta$ -unsaturated ketones.<sup>2</sup> Thus, we decided to explore these challenging substrates, first focusing on cyclohexenone derivatives. Preliminary investigations identified trifluoroacetic acid salts of the cinchona alkaloid-derived amine **1a** as powerful catalysts for the epoxidation of cyclohexenone **9a** with aqueous hydrogen peroxide. As with acyclic enones, the optimal reaction medium proved to be 1,4-dioxane at 50 °C. Using the optimized conditions, the scope of the epoxidation was

explored using various substituted cyclohexenones (Table 4). It is noteworthy that initial products of hydroperoxidation could not be detected with any of the substrates **9**. Simple

Table 4. Catalytic Asymmetric Epoxidation of Cyclohexenone Derivatives



entry	substrate	product	yield, [%]	er <sup>a</sup>
1		<b>9a</b> <b>10a</b>	58 (93)	97:3
2		<b>9b</b> <b>10b</b>	84	97:3
3		<b>9c</b> <b>10c</b>	72	96:4
4		<b>9d</b> <b>10d</b>	52	95.5:4.5
5 <sup>b,c</sup>		<b>9e</b> <b>10e</b>	49 <sup>d</sup>	96:4
6 <sup>c</sup>	R = Me	<b>9f</b> <b>10f</b>	70	98:2
7	Et	<b>9g</b> <b>10g</b>	73	98.5:1.5
8	<i>i</i> -Bu	<b>9h</b> <b>10h</b>	73	98:2
9	<i>i</i> -Pr	<b>9i</b> <b>10i</b>	79	99:1
10	<i>t</i> -Bu	<b>9j</b> <b>10j</b>	68	99.5:0.5
11	allyl	<b>9k</b> <b>10k</b>	23	97.5:2.5
12	CH <sub>2</sub> CH <sub>2</sub> Ph	<b>9l</b> <b>10l</b>	84	98.5:1.5
13	CH <sub>2</sub> Ph	<b>9m</b> <b>10m</b>	78	99:1
14 <sup>f</sup>	CH <sub>2</sub> Ph	<b>9m</b> <b>ent-10m</b>	77	98.5:1.5
15	Ph	<b>9n</b> <b>10n</b>	0	-
16	vinyl	<b>9o</b> <b>10o</b>	0	-
17	ethynyl	<b>9p</b> <b>10p</b>	0	-
18		<b>9q</b> <b>10q</b>	94 <sup>g</sup>	93.5:6.5 (anti) 99:1 ( <i>syn</i> )
19		<b>9r</b> <b>10r</b>	75	98.5:1.5 <sup>h</sup>

<sup>a</sup>Determined by GC with a chiral stationary phase. The absolute configuration (2*S*,3*S*) of **10a** was determined from its known optical rotation.<sup>31</sup> <sup>b</sup>Performed at 50 °C. <sup>c</sup>Performed using 20 mol % catalyst salt [1a:2 TFA]. <sup>d</sup>54% conversion determined by GC. <sup>e</sup>Performed at 30 °C for 24 h. <sup>f</sup>Performed using catalyst **1b** (10 mol %). <sup>g</sup>GC-conversion, dr = 54:46 (*anti:syn*). <sup>h</sup>dr = 97:3 (*anti:syn*).

cyclohexenone (entry 1) and substrates bearing substituents at the 4-position (entry 2), 5-position (entry 3), and 3-position were all equally well tolerated, giving the corresponding epoxide products with excellent enantioselectivities and good yields. Diketone **9e** (entry 5) proved to be less reactive but nevertheless gave the corresponding epoxide **10e** in a reasonable yield along with high enantioselectivity of 96:4 er.

We next examined the effect of substituents at the 3-position. Substrates bearing a variety of linear and branched alkyl substituents underwent epoxidation smoothly with good yields and excellent enantioselectivity (entries 6–14). Using the pseudoenantiomeric catalyst **1b**, the opposite enantiomer of product **10m** could be efficiently obtained from substrate **9m** (entry 14). A diminished yield (23%) was obtained with substrate **9k** bearing an allyl substituent (entry 11). Partial isomerization of the terminal double bond into conjugation with the  $\alpha,\beta$ -enone moiety was observed for this substrate, giving an unreactive dienone.<sup>32</sup>

Extended conjugation of the double bond was not tolerated in the reaction, with phenyl, vinyl and ethynyl substituents rendering enones **9n–p** unreactive (entries 10–12). In addition, 2-substituted cyclic enones represent a limitation of the method.

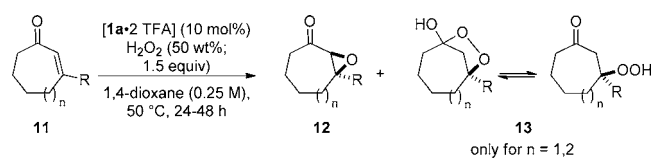
We were also intrigued by the possibility of a (dynamic) kinetic resolution of racemic 4-substituted or enantiopure 5-substituted cyclohexenones via asymmetric epoxidation. Employing 4-methyl substituted enone *rac*-**9q**, however, we observed the formation of both diastereomeric epoxides *syn*- and *anti*-**10q** with high enantioselectivities at similar rates (entry 18). In stark contrast, the racemic synthesis with alkaline hydrogen peroxide in methanol proceeded with a diastereoselectivity of 74:26 dr in favor of the *anti*-epoxide **10q**.<sup>33</sup>

We further wished to probe the effect of pre-existing stereocenters embedded in the ring scaffold, which cannot be equilibrated in the course of the reaction. To this end, we prepared enantioenriched 5-phenyl-3-methyl-2-cyclohexenone (*S*)-**9r** according to a method previously developed by our group.<sup>34</sup> Subjecting this substrate to our standard epoxidation conditions delivered epoxide *anti*-**10r** featuring three stereogenic centers with excellent yield, diastereoselectivity and enantioselectivity (entry 19).

**Epoxidation of Cyclic Enones: Medium<sup>8c</sup> and Large-Sized Rings.** Having identified a robust epoxidation procedure for cyclohexenone derivatives, we turned our attention to medium- and large-sized cyclic enones **11** (Table 5). Gratifyingly, 7–15-membered cycloalkenones all underwent epoxidation with good to excellent yields and outstanding enantioselectivities. Moreover, the use of the pseudoenantiomeric catalyst **1b** enabled facile synthesis of enantiomeric product *ent*-**12f** with equal efficiency (entry 9). These results raise the intriguing possibility of effecting stereoselective, catalyst-controlled late-stage epoxidation of macrocyclic cores for natural product synthesis,<sup>35</sup> especially given the stereoconvergent nature of our method.

Whereas epoxides were the only products observed in the **1a**-catalyzed reaction of cyclohexenones **9** with hydrogen peroxide, optically active peroxidic side products **13** could be detected with larger ring-sized enones **11**, analogously to the acyclic  $\alpha,\beta$ -unsaturated ketones **2**. In contrast to products **3**, which overwhelmingly exist as cyclic peroxyhemiketals, mixtures of monocyclic  $\beta$ -hydroperoxyketone and bicyclic peroxyhemiketal forms of **13** could be detected in solution by NMR for the seven- and eight-membered substrates. Based on this

**Table 5. Catalytic Asymmetric Epoxidation of Medium and Large Ring-Sized Enones**



entry	substrate	product	yield, [%]	er <sup>a</sup>
1		<b>11a</b>	<b>12a</b> 62	>99.5:0.5
2 <sup>b</sup>		<b>11a</b>	<b>13a</b> 89 <sup>c</sup>	99:1
3		<b>11b</b>	<b>12b</b> 82	>99.5:0.5
4		<b>11c</b>	<b>12c</b> 82	>99.5:0.5
5 <sup>d</sup>		<b>11d</b>	<b>12d</b> 55	98:2
6		<b>11d</b>	<b>13d</b> 91 <sup>c</sup>	>99.5:0.5
7		<b>11e</b>	<b>12e</b> 92	99.5:0.5
8		<b>11f</b>	<b>12f</b> 87	99.5:0.5
9 <sup>f</sup>		<b>11f</b>	<i>ent</i> - <b>12f</b> 86	99.5:0.5

<sup>a</sup>Determined by GC with a chiral stationary phase. <sup>b</sup>alternative conditions: [**1a-2** TCA] (10 mol %), H<sub>2</sub>O<sub>2</sub> (30 wt %; 3 equiv), 1,4-dioxane (0.25 M), 32 °C, 20 h. <sup>c</sup><sup>1</sup>H NMR conversion, **12a**:**13a** = 23:77 <sup>d</sup>Performed at 50 °C. Crude product was treated with 1N NaOH (1 equiv) in THF. <sup>e</sup><sup>1</sup>H NMR conversion, **12d**:**13d** = 12:88. <sup>f</sup>Using catalyst **1b**.

observation we speculate that an internal hydrogen bond can be established in medium-sized rings, which stabilizes the  $\beta$ -hydroperoxyketone form.

The hydroperoxidation/epoxidation product distribution was found to strongly depend on the ring size of the cycloalkenones. While the smallest ( $n < 7$ ) and the largest ( $n \geq 12$ ) ring sizes significantly favored epoxidation, eight-membered 2-cyclooctenone **11d** provided peroxide **13d** as the major product (yield of epoxidation product: blue, yield of peroxidation product: red, Figure 1). Even though data for the ring sizes 9–11 are not available, the amount of hydroperoxide product



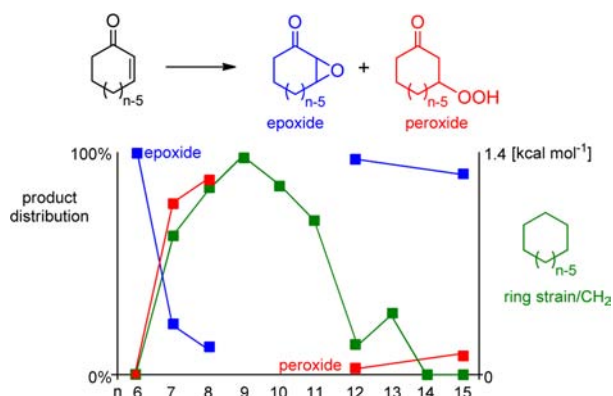


**Figure 1.** Hydroperoxidation/epoxidation product distribution of cyclic enones of varying ring size and ring strain/CH<sub>2</sub> of the corresponding cycloalkanes.<sup>36</sup>

obtained seems to correlate with the ring strain found in the corresponding cycloalkanes (green). As with peroxyhemiketals **3**, peroxidic products **13** could be transformed to the corresponding epoxides **12** by a simple aqueous NaOH workup.

Peroxides **13a** and **13d**, derived from 2-cycloheptenone (**11a**) and 2-cyclooctenone (**11d**), respectively, piqued our interest since their bicyclic peroxidic structure resembles potent antimalarial agents and since both compounds have not been previously described in the literature. With the goal of optimizing the yield of the peroxidic products at the expense of the corresponding epoxides, we evaluated various reaction parameters. Gratifyingly, the product ratio could be shifted in favor of the peroxidation products by simply switching the acid cocatalyst to trichloroacetic acid and employing less concentrated aqueous hydrogen peroxide (Table 5, entries 2 and 6).

We presume that conformational constraints in the seven- and eight-membered ring systems, in contrast to 2-cyclohexenone, may hamper the peroxyenamine intermediate in adopting the proper conformation for epoxide ring closure, which requires an antiperiplanar alignment of the  $\pi$ -system of the enamine with the O–O single bond. These difficulties might be reflected in the accumulation of hydroperoxidation product **13** over the course of the reaction. In contrast, large rings are very flexible and show complex conformational behavior. As a result, cyclododecenone **11e** and cyclopentadecenone **11f** provide almost exclusively the corresponding  $\alpha,\beta$ -epoxyketones **12** under both sets of conditions.

As with the acyclic epoxides **4**, we wished to demonstrate the synthetic utility of cyclic epoxides **12** by reducing them to aldol-like products **15**.<sup>37</sup> This was achieved by the previously established method employing *in situ* generated phenyl selenide (Table 6). The resulting six- to eight-membered cyclic hydroxyketones **15a–d** were obtained in good to excellent yields and enantioselectivities. The method also proved effective for the generation of a highly enantioenriched quaternary oxygenated stereocenter (entry 2). It should be noted that none of these compounds had been accessed through a catalytic asymmetric methodology prior to our work. The synthesis of seven- and eight-membered products **15c** and **15d** is particularly valuable in light of the fact that these compounds cannot be accessed via an intramolecular aldol disconnection, as the required keto-aldehydes preferentially form six-membered cyclic aldol products through enoloxo-

**Table 6.** Asymmetric Synthesis of Cyclic  $\beta$ -Hydroxyketones

entry	product	yield, [%]	er <sup>a</sup>	
1		<b>15a</b>	94	96:4
2		<b>15b</b>	87	95.5:4.5
3		<b>15c</b>	84	99:1
4		<b>15d</b>	53	86:14

<sup>a</sup>Determined by GC with a chiral stationary phase.

aldolizations rather than the seven- or eight-membered cyclic products through enolendo-aldolizations.<sup>38</sup>

#### Epoxidation of Cyclic Enones: Cyclopentenones.<sup>8h</sup>

Despite the generality of our method for enone substrates with small, medium, and large rings, the epoxidation of cyclopentenones **16** proved to be a considerable challenge. Indeed, the substantial “flatness” of these small rings, which presumably renders them less sensitive to the steric requirements of a chiral catalyst, makes 2-cyclopentenones a notoriously difficult substrate class for iminium-catalyzed asymmetric conjugate additions.<sup>39</sup> We have recently identified a new class of cinchona-derived primary amine catalysts bearing a C2'-substituent on the quinoline group, which enabled us to develop the first asymmetric catalytic Knoevenagel condensation.<sup>8g</sup> Inspired by these results, we decided to explore this catalyst class in the asymmetric epoxidation. Quinoline C2'-substituted cinchona amines are readily accessible via a protecting group-free one-pot procedure consisting of addition of an organometallic reagent followed by oxidation. Careful optimization identified amine **1c** together with Mosher's acid **18** as a powerful catalyst salt for the enantioselective epoxidation of cyclopentenones.<sup>40</sup> As in the previous systems, 1,4-dioxane remained the solvent of choice, albeit the temperature had to be lowered to room temperature to achieve the best enantioselectivity. With the optimal conditions in hand, the scope of the epoxidation was explored (Table 7). To our delight, simple 2-cyclopentenone (entry 1) as well as its derivatives bearing a variety of linear and branched substituents in the 3-position (entries 2–4) and 4-position (entry 5) could be converted to the corresponding epoxy cyclopentenones **17** with excellent yields and enantioselectivities.

**Epoxidation of  $\alpha$ -Branched Enals.<sup>8e</sup>** Despite the existence of several methodologies for the nonasymmetric epoxidation of  $\alpha$ -branched enals,<sup>2e,41</sup> direct catalytic enantioselective variants for this transformation were lacking at the outset of our studies.<sup>42</sup> Encouraged by the success of catalyst **1a** in the epoxidation of various enones, we reasoned that the similar steric requirements of  $\alpha$ -branched enals might make them a suitable substrate class for our developed catalytic system. Our expectations were further supported by recent

Table 7. Catalytic Asymmetric Epoxidation of Substituted 2-Cyclopentenones

entry <sup>a</sup>	substrate	product	yield, [%] <sup>b</sup>	er <sup>b</sup>
1			87	95:5
2			89	95.5:4.5
3			65	96:4
4			84	97.5:2.5
5			90	96.5:3.5

<sup>a</sup>Performed on 0.2 mmol scale. <sup>b</sup>Determined by GC with a chiral stationary phase.

reports, which demonstrated that  $\alpha$ -branched enals could be efficiently activated for asymmetric transformations by primary amine catalysts.<sup>9a,43</sup>

Indeed, applying the conditions optimized for enones **2** to the epoxidation of (*E*)-2-methylpent-2-enal **19a**, we were pleased to obtain the desired epoxide **20a** with a significant enantiomeric ratio of 93:7, albeit with a modest chemical yield. Starting from the (*E*)-configured enal **19a**, the epoxide **20a** was formed as a mixture of diastereomers with moderate *trans*-selectivity of 75:25. As with five- and six-membered cyclic enones, products of initial hydroperoxidation could not be detected in the reaction.

Optimization of the catalyst system revealed a very strong effect of the acid cocatalyst on the enantio- and diastereoselectivity of the reaction, indicating a possible involvement of the iminium counteranion in enantiodiscrimination.<sup>3c</sup> Remarkably, applying the chiral phosphoric acid (*R*)-TRIP ((*R*)-**21a**) as the acid cocatalyst, we observed a dramatic case of “matched” asymmetric induction, whereby the product **20a** was obtained in essentially enantiopure form (er = 99.5:0.5). Using the (*S*)-enantiomer of TRIP resulted in the loss of synergism, giving a reversed but modest enantioselectivity of 36:64.<sup>8c</sup> After further optimization to improve the yield, we found that the phenyl-substituted BINOL-derived phosphoric acid (*R*)-**21b** formed a more active but equally enantioselective catalyst salt [**1a**·2 (*R*)-**21b**]. Using the optimized conditions, we examined the scope of the asymmetric epoxidation (Table 8). Excellent enantioselectivity and good diastereoselectivity and yields were observed for all substrates, regardless of the size of the  $\alpha$ -substituent (entries 1–3). Cyclic substrate **19d** (entry 4) and enal **19f** bearing an ester group (entry 6) underwent the epoxidation smoothly. In contrast to enones **2**, enals bearing aromatic substituents in conjugation with the double bond (entries 5 and

Table 8. Catalytic Asymmetric Epoxidation of  $\alpha,\beta$ -Disubstituted Enals

entry <sup>a</sup>	substrate	product	yield, [%] <sup>b</sup>	dr <sup>c</sup>	er <sup>d</sup>
1	<b>19a</b>	<b>20a</b>	43	92:8	98.5:1.5
2	<b>19b</b>	<b>20b</b>	64	83:17 <sup>e</sup>	99:1
3	<b>19c</b>	<b>20c</b>	77	90:10	99:1
4	<b>19d</b>	<b>20d</b>	70	>99:1	98.5:1.5
5 <sup>f</sup>	<b>19e</b>	<b>20e</b>	49	97:3	98:2
6	<b>19f</b>	<b>20f</b>	66	93:7	99:1
7	<b>19g</b>	<b>20g</b>	75	95:5	98.5:1.5
8	<b>19h</b>	<b>20h</b>	49 <sup>g</sup>	56:44	95:5
9	<b>19i</b>	<b>20i</b>	30	95:5	70:30

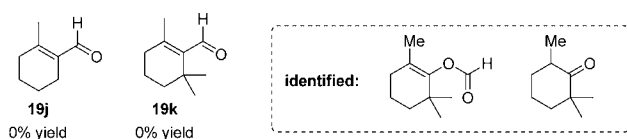
<sup>a</sup>All reactions performed on 0.25 mmol scale. <sup>b</sup>Yields refer to isolated yields after NaBH<sub>4</sub> reduction. <sup>c</sup>Determined by GC of the crude reaction mixture. <sup>d</sup>Determined by GC with a chiral stationary phase. The absolute configuration (2*R*,3*S*) of **19a** was assigned by comparing the optical rotation of the corresponding alcohol to the literature value.<sup>44</sup> <sup>e</sup>Opposite diastereoselectivity (28:72 dr) in the racemic reaction using alkaline hydrogen peroxide. <sup>f</sup>48 h reaction time, low yield due to incomplete conversion. <sup>g</sup>Unidentified side product also isolated.

8) were also suitable, although a phenyl  $\alpha$ -substituent resulted in the erosion of diastereoselectivity (entry 8). Interestingly, the primary amine catalytic platform proved unsuitable for the  $\alpha$ -unbranched enal **19i**, affording the corresponding product **20i** with the opposite absolute configuration and only modest enantioselectivity and yield (entry 9).

Substrates containing a tetrasubstituted double bond (enals **19j** and **19k**) proved unreactive toward epoxidation, presumably due to difficulties of the amine catalyst in condensing with the sterically hindered aldehyde moiety. Instead, decomposition products via Baeyer–Villiger and Dakin-type reactions were observed (Scheme 6).

We also tested the reaction for stereoconvergence by submitting the (*Z*)-configured enal **19g** to the epoxidation



Scheme 6. Current Limitations in the Epoxidation of  $\alpha$ -Branched Enals

conditions and found that the reaction proceeds by a stereoconvergent mechanism.<sup>17</sup>

We next turned our attention to the epoxidation of a related substrate class, the 2-substituted acroleins **22**. Initial investigations using the TFA salt of cinchona amine **1a** as the catalyst revealed only very low asymmetric induction (59:41 er) for this substrate, in stark contrast to the  $\alpha,\beta$ -disubstituted enal **2a** (93:7 er). Because conjugate addition of hydrogen peroxide to the unsubstituted  $\beta$ -carbon of enals **22** does not produce a stereogenic center, the subsequent epoxide ring closure of the peroxyenamine intermediate must constitute the enantiodetermining step of the reaction. The different mechanistic regimes, which are likely responsible for the enantiodetermining steps in the epoxidation of enals **19** and **22** may thus explain the drastic difference in the enantioselectivity of their epoxidation by the TFA salt of cinchona amine **1a**.

Gratifyingly, we found that using the chiral acid cocatalyst (*R*)-**21b** dramatically increased the enantioselectivity of the reaction to 91:9 er, which could be further improved to 99:1 er by using the bulkier phosphoric acid (*R*)-TRIP ((*R*)-**21a**). Using the optimized conditions, we screened various acrolein derivatives **22** and observed excellent enantioselectivity and good yields for all tested substrates (Table 9).

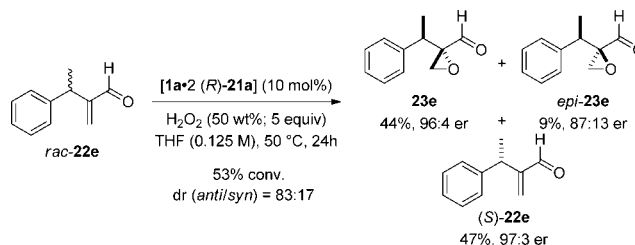
Table 9. Catalytic Asymmetric Epoxidation of 2-Substituted Acroleins

entry <sup>a</sup>	substrate	product	yield, [%] <sup>b</sup>	er <sup>c</sup>
1	<b>22a</b>	<b>23a</b>	78 <sup>d</sup>	99:1
2	<b>22b</b>	<b>23b</b>	74	98.5:1.5
3	<b>22c</b>	<b>23c</b>	29 <sup>e</sup>	98:2
4	<b>22d</b>	<b>23d</b>	84	99:1

<sup>a</sup>All reactions performed on 0.25 mmol scale. <sup>b</sup>Isolated yields after NaBH<sub>4</sub> reduction. <sup>c</sup>Determined by GC with a chiral stationary phase. <sup>d</sup>Isolated yield of the aldehyde. <sup>e</sup>The decreased yield reflects the high volatility of the product.

Diminished yield for substrate **22c** (entry 3) reflects the high volatility of the corresponding product **23c**. Applying the pseudoenantiomeric form of the amine catalyst **1b** and (*S*)-**21a** as the catalytic salt in the epoxidation of **22a** provided the corresponding (*S*)-product *ent*-**23a** with only 44% yield and a modest enantioselectivity of 71:29 er. However, complementary approaches, which furnish the (*S*)-products with high enantiomeric excess, were recently reported by the groups of Hayashi<sup>7a</sup> and Luo.<sup>11d</sup>

The catalytic system [**1a**·2 (*R*)-**21a**] also proved to be highly efficient in a kinetic resolution of a  $\beta'$ -substituted enal *rac*-**22e** (Scheme 7).

Scheme 7. Kinetic Resolution of *rac*-**22e** by Asymmetric Epoxidation

Under the standard reaction conditions, the reaction proceeded to 53% conversion, whereby (*R*)-**22e** underwent a highly selective epoxidation, while (*S*)-**22e** was recovered with 97:3 er.

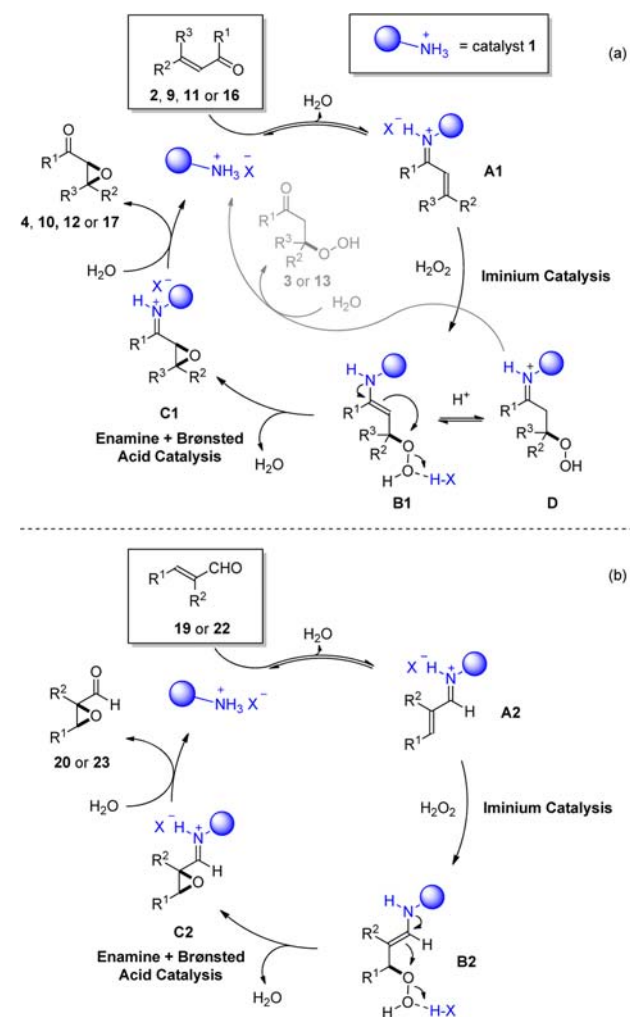
**Mechanistic Aspects.** We propose that all of our epoxidation reactions proceed via the same general mechanism of iminium ion-catalyzed oxa-Michael addition of hydrogen peroxide followed by epoxide ring closure of the resulting peroxy enamine (Scheme 8), analogously to the well-studied mechanism of the Weitz–Scheffer epoxidation.<sup>4</sup>

In particular, the initial formation of the  $\alpha,\beta$ -unsaturated iminium ion **A1** (derived from enones) or **A2** (derived from enals) promotes a nucleophilic attack by hydrogen peroxide, forming the corresponding  $\beta$ -peroxyenamine intermediate **B1**/**B2**. Protonation of **B1** to give iminium **D** followed by hydrolysis gives hydroperoxides **3**/**13**, which can be considered as products of “interrupted epoxidation” (Scheme 8a). As described in the previous sections, the stability of such products appears to be substrate specific and their isolation limited to acyclic,<sup>8e</sup> medium ring-sized ( $n = 7,8$ ) and macrocyclic ( $n > 12$ ) enones. In contrast, no hydroperoxide intermediates could be isolated with enals, cyclopentenones, and cyclohexenones. A combination of enamine and Brønsted acid catalysis is believed to promote the ring closure of **B1**/**B2** to the epoxide intermediate **C1**/**C2**.<sup>45</sup> Subsequent hydrolysis liberates the epoxide product and regenerates the catalyst.

An important difference from the Weitz–Scheffer epoxidation concerns the reversibility of the oxa-Michael addition of hydrogen peroxide (step **A**→**B**, Scheme 8). The basic conditions of Weitz–Scheffer epoxidations create a hydroperoxide anion as the active nucleophile, whose addition to unsaturated carbonyls has been confirmed by kinetic data to be fast and reversible.<sup>38d,38e</sup> Under our reaction conditions in the presence of catalyst salts, which include 2 equiv of a Brønsted acid, neutral hydrogen peroxide rather than the hydroperoxide anion is expected to be the active nucleophile. Consequently, the conjugate addition is most likely irreversible and constitutes the enantiodetermining step of the catalytic cycle.<sup>46</sup> This is supported by the high enantiomeric excess of the isolable hydroperoxy intermediates **3** and **13** (er >95:5), which would be expected to be racemic under a reversible mechanistic regime.<sup>47</sup>

To provide comprehensive support for the proposed mechanism and to elucidate the origin of enantioselectivity, we performed mechanistic studies on both enone and enal substrates, employing various experimental and computational approaches.

Scheme 8. Proposed Catalytic Cycles for the Epoxidation of Enone and Enal Substrates with Catalysts 1



### Structure–Activity Relationship of Modified Catalyst

**1a.** We first verified that the presence of the primary amine moiety in **1a** is indeed crucial for the observed reaction rate and enantioselectivity, supporting a mechanism proceeding through iminium activation and not via other activation modes, such as general base catalysis or phase-transfer catalysis.<sup>48</sup> This is further corroborated by the complementarity of scope observed in reactions catalyzed by **1a** and in phase transfer catalysis. While steric congestion around the carbonyl group (e.g.,  $\alpha$ -substituents in the cyclohexenone series) is detrimental in our reactions, an opposite effect is observed under phase-transfer catalysis in comparable systems.<sup>49</sup>

**ESI-MS Studies and Catalyst N-Oxidation.** To provide further support for covalent catalytic intermediates and to follow the fate of the amine catalyst **1a**, we performed electrospray ionization mass spectroscopy (ESI-MS) studies using the epoxidation of acyclic enone **2a** as a model system (Scheme 9). Samples of the crude reaction mixture taken at various time points over 24 h were analyzed, and the selected spectra are shown in Scheme 18 in the Supporting Information.<sup>17</sup> The ESI(+)-MS spectrum of a sample taken prior to the addition of hydrogen peroxide (Scheme 9a) revealed the characteristic signals corresponding to the amine catalyst **1a** at  $m/z$  324 ( $[\mathbf{1a}+\text{H}]^+$ ) as well as iminium ion **A** at  $m/z$  460, formed by the condensation of the amine **1a** and

enone **2a**. After H<sub>2</sub>O<sub>2</sub> addition (Scheme 9), iminium ion **A** could no longer be detected, suggesting its rapid consumption by hydrogen peroxide, although the signal for the free catalyst **1a** remained. Already after 1 h reaction time, two new peaks could be detected at  $m/z$  476 and at  $m/z$  494 which match the masses of the iminium ion **B** derived from 2,3-epoxy-2-decanone (**4a**) and iminium ion **C** derived from the corresponding  $\beta$ -hydroperoxyketone, which upon hydrolysis affords peroxyhemiketal **3a**. LRMS and HRMS data obtained for catalyst **1a** and intermediates **A–C** are summarized in Table 10.

The fact that the free catalyst **1a** as well as the intermediate products of hydroperoxidation (**B**) and intramolecular epoxide closure (**C**) could be easily detected under the reaction conditions, while the iminium ion **A** remained below the detection limit, suggests that the initial formation of the iminium intermediate **A** could be the rate-limiting step of the reaction.<sup>17</sup>

When analyzing the reaction at 50 °C, we were particularly intrigued by the appearance of additional signals at  $m/z$  340, 492, and 510, which presumably correspond to the oxidized catalyst (species **1a<sub>+O</sub>**) and iminium ions **B<sub>+O</sub>** and **C<sub>+O</sub>** that incorporate this oxygenated catalyst (Scheme 9b and Table 10). After 12 h of reaction time, these peaks gained in intensity, while the parent peaks **1a**, **B** and **C** ( $m/z$  324, 476 and 494, respectively) showed considerable loss of intensity, suggesting catalyst oxidation.<sup>17</sup> It is noteworthy that a doubly oxidized catalyst species, i.e. a mass incorporating two oxygens ( $m/z$  356) could not be detected.

Since all of the reactions with the amine catalyst **1a** proceed to completion and the epoxidation products are formed with outstanding enantioselectivities, the observed *in situ* oxidation of the catalyst raised interesting mechanistic questions. Specifically, we wondered if the oxidized catalyst **1a<sub>+O</sub>** is active, and hence if the iminium ions **B<sub>+O</sub>** and **C<sub>+O</sub>** are catalytically relevant intermediates. Their formation suggested to us that the primary amine functionality of the catalyst **1a** cannot be involved in the oxidation to **1a<sub>+O</sub>**. We therefore hypothesized that species **1a<sub>+O</sub>** most likely arises from the N-oxidation of the most nucleophilic quinuclidine nitrogen. Toward this end, we synthesized 9-amino(9-deoxy)epiquinine N-oxide **24** using *m*-CPBA (Scheme 10) and could unambiguously confirm the site of N-oxidation by <sup>15</sup>N-HMBC analysis.<sup>17</sup>

With an authentic sample of **24** in hand, we next analyzed the catalyst species, which remained at the end of the epoxidation reaction shown in Scheme 9. Although analysis of the crude reaction revealed a complex mixture of compounds containing the quinine scaffold, which presumably correspond to various catalytic intermediates, direct elution on silica gel allowed us to isolate a single species of significantly higher polarity. Characterization of this product confirmed it to be identical to **24**. In addition, when we submitted **1a** to the standard conditions of epoxidation in the absence of any enone substrate, we observed a clean and quantitative formation of the bis-trifluoroacetic acid salt of **24**.

Having thus established the identity of **1a<sub>+O</sub>** as the N-oxide **24**, we examined its chemical reactivity. Oh and Ryu have recently shown that tertiary amine N-oxides can act as oxygen transfer agents to effect asymmetric epoxidation of enones at 100 °C.<sup>50</sup> However, mixing an excess (1.5 equiv) of **24** with enone **2a** in the absence of hydrogen peroxide at 50 °C did not give any oxidation products, ruling out the ability of **24** to act as an oxidant under our standard reaction conditions.

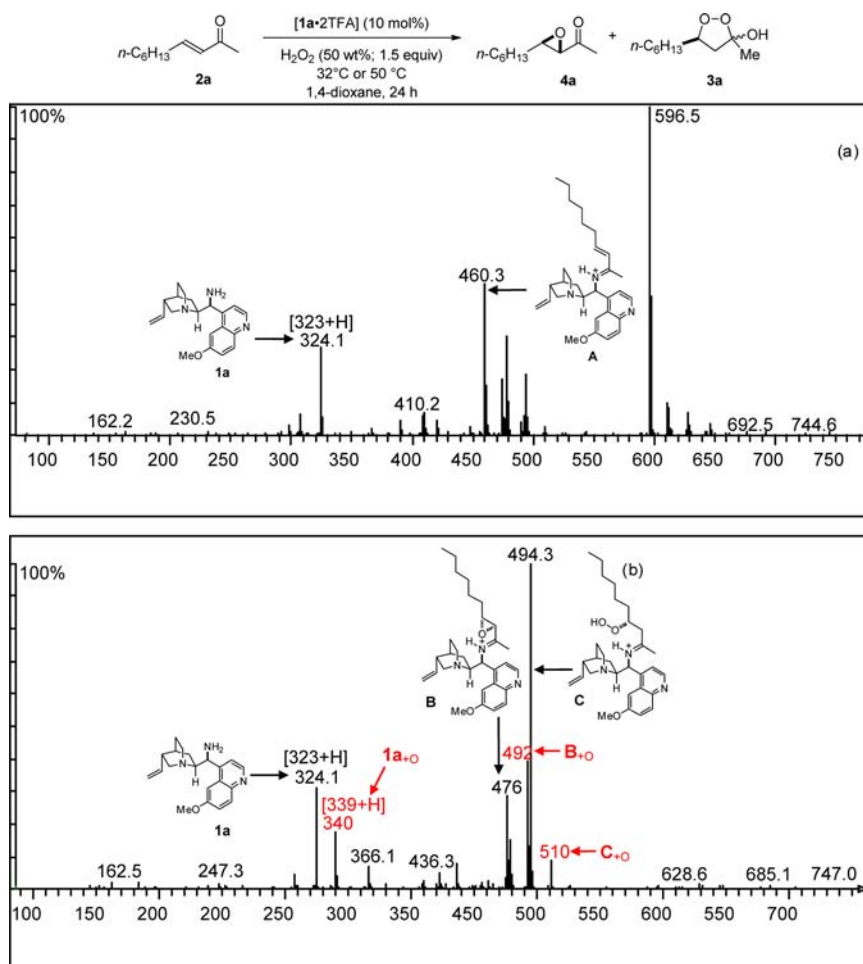
Scheme 9. ESI(+)-MS Studies on the Epoxidation and Hydroperoxidation of 2a: (a) Spectrum of the Reaction Sample Recorded (a) Prior to H<sub>2</sub>O<sub>2</sub> Addition and (b) at 50 °C after 1 h

Table 10. Low- and High-Resolution Mass Spectrometric Analysis of Catalytic Species in the Epoxidation of Enone 2a

species					$[1a_{+O}+H]$	$B_{+O}$	$C_{+O}$
	$[1a+H]^+$	A	B	C			
formula	C <sub>20</sub> H <sub>26</sub> N <sub>3</sub> O	C <sub>30</sub> H <sub>42</sub> N <sub>3</sub> O	C <sub>30</sub> H <sub>42</sub> N <sub>3</sub> O	C <sub>30</sub> H <sub>44</sub> N <sub>3</sub> O <sub>3</sub>	C <sub>20</sub> H <sub>26</sub> N <sub>3</sub> O <sub>2</sub>	C <sub>30</sub> H <sub>42</sub> N <sub>3</sub> O <sub>3</sub>	C <sub>20</sub> H <sub>26</sub> N <sub>3</sub> O
LRMS	324.1	460.3	476	494.3	340	492	510
HRMS							
found	324.207039	460.332803	476.327879	494.338147	340.201945 <sup>a</sup>	492.322675	-
calcd	324.206741	460.332238	476.327145	494.337720	340.201953	492.322065	-
deviation	0.92	1.23	1.52	0.86	0.02	1.24	-
[ppm]							

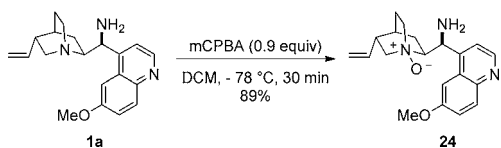
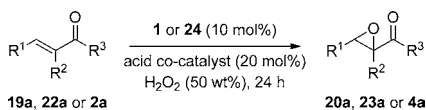
<sup>a</sup>HRMS of purified 2a.

We next investigated the competence of **24** as a catalyst, submitting it to the epoxidation reactions of enals **19a**, **22a**, and enone **2a** under the corresponding optimized conditions for each substrate, along with a control reaction using amine **1a** (Table 11).

After 24 h, all substrates underwent epoxidation with a comparable conversion using either catalyst, suggesting that the

amine **24** is catalytically active. Furthermore, when using amine **24**, epoxides **20a**, **23a**, and **4a** were formed with the same sense of stereoselection and similar enantio- and diastereoselectivity as with catalyst **1a**. These findings suggest that the *in situ* N-oxidation of catalyst **1a** creates a small amount of a different, but similarly competent catalytic species, which might catalyze the reaction in parallel with **1a**, explaining the high



Scheme 10. Synthesis of an Authentic Sample of 9-Amino(9-deoxy)epiquinine *N*-Oxide 24Table 11. Catalytic Activity of *N*-Oxide 24

19a, 20a: R<sup>1</sup> = Et, R<sup>2</sup> = Me, R<sup>3</sup> = H  
 22a, 23a: R<sup>1</sup> = H, R<sup>2</sup> = CH<sub>2</sub>Ph, R<sup>3</sup> = H  
 2a, 4a: R<sup>1</sup> = *n*-C<sub>6</sub>H<sub>15</sub>, R<sup>2</sup> = H, R<sup>3</sup> = Me

entry	amine catalyst	acid cocatalyst	product	yield [%] <sup>a,c</sup>	dr <sup>b</sup>	er <sup>b,d</sup>
1	1a	( <i>R</i> )-21b	20a	94	93:7	99:1 ( <i>R,S</i> )
2	24	( <i>R</i> )-21b	20a	99.5	86:14	97.5:2.5 ( <i>R,S</i> )
3	1a	( <i>R</i> )-21a	23a	97	—	99:1 ( <i>R</i> )
4	24	( <i>R</i> )-21a	23a	90	—	94:6 ( <i>R</i> )
5	1a	TFA	4a	99	>99:1	98.5:1.5 ( <i>S,R</i> )
6	24	TFA	4a	83	>99:1	96.5:3.5 ( <i>S,R</i> )

<sup>a</sup>Determined by <sup>1</sup>H NMR analysis. <sup>b</sup>Determined by GC with a chiral stationary phase. <sup>c</sup>Refers to the GC yield of the product 20a, 23a, or 4a. <sup>d</sup>Refers to the er of the epoxide product 20a (major diastereomer), 23a or 4a (after 1 N NaOH workup). See Tables 2, 8, 12 for precise reaction conditions. TFA = trifluoroacetic acid.

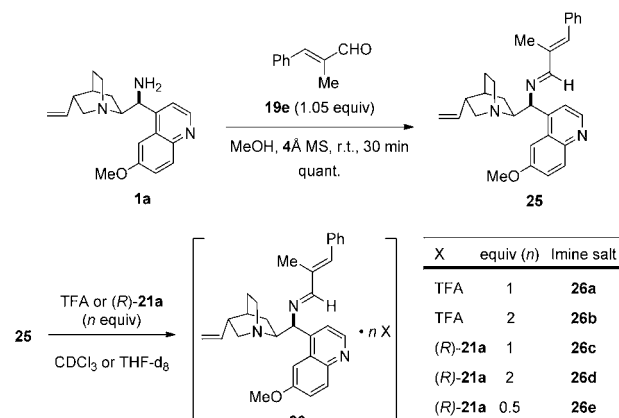
enantioselectivity maintained throughout our epoxidation reactions and complete conversion of the starting materials.

**Origin of Enantioselectivity.** Despite the myriad of synthetic transformations employing catalyst 1a and its related cinchona-based congeners reported in recent years, only a single computational investigation has attempted to rationalize the origin of enantioselectivity imparted by this versatile catalytic platform.<sup>51</sup> A number of methodological reports have speculated on the role of the quinuclidine moiety in catalyst 1a suggesting that it acts as a free base in the transition state (TS), coordinating the weakly acidic hydrogen peroxide.<sup>5b,c,8e,45</sup> Yet our findings of the excellent catalytic performance by the *N*-oxidized catalyst 24 in which the quinuclidine nitrogen is replaced with a weakly basic *N*-oxide moiety<sup>52</sup> raised intriguing mechanistic questions. We decided to investigate the mechanism of facial selectivity by 1a using a combination of conformational analysis of catalytic intermediates and computational techniques.

As outlined earlier, experimental evidence suggested that the conjugate addition of hydrogen peroxide constitutes the enantiodetermining step of our epoxidation reactions. We therefore chose to investigate the chiral iminium adducts **A**, which are formed by the reversible condensation of catalyst 1a with the carbonyl substrate, and act as acceptors in the first C–O bond-forming conjugate addition (Scheme 8). Toward this end, we found that  $\alpha$ -branched enals **19** provide a useful model system, undergoing smooth condensation with amine 1a in the presence of 4 Å molecular sieves. Using enal **19e** in a slight (5%) excess to ensure complete consumption of 1a, the corresponding imine **25** could be isolated without purification as a bench-stable amorphous solid containing traces of the remaining **19e** (Scheme 11). Employing strictly anhydrous

conditions, we could also prepare stable solutions of iminium salts **26** containing 0.5–2 equivalents of Brønsted acids TFA and (*R*)-TRIP ((*R*)-21a).

## Scheme 11. Synthesis of Imine 25 and Iminium Salts 26



Unfortunately, extensive attempts to crystallize **25** or its various salts did not meet with success. However, a combination of solution-state NMR and DFT calculations allowed for a detailed characterization and conformational assignment of imine **25** and its salts **26**.<sup>17</sup> Figure 2a represents

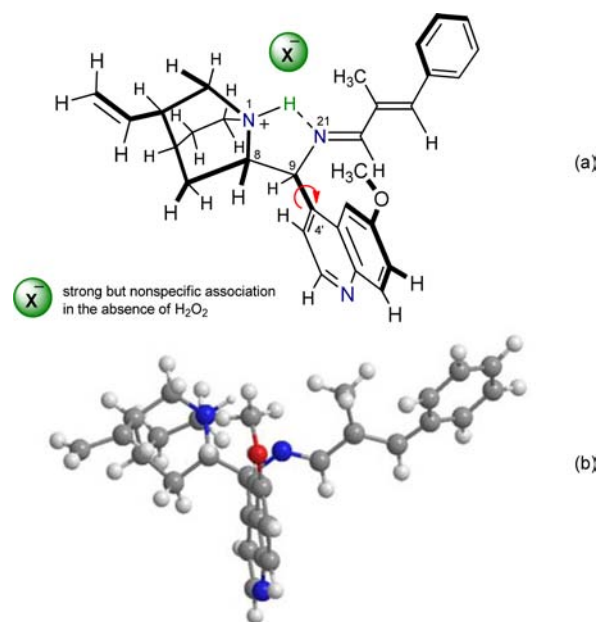


**Figure 2.** Structure of the monoprotonated iminium **26** elucidated by NMR techniques (a) and gas-phase density functional calculations (B3LYP/SVP) (b).

the structural features of the monoprotonated iminium **26** obtained by NMR analysis, which was found to be in excellent agreement with an energy-minimized structure derived by DFT calculations (Figure 2b).

Similarly to the parent cinchona alkaloids,<sup>53</sup> imine **25** was found to have a strong conformational preference in solution, which was further rigidified by protonation. Analysis of salts **26a–e** revealed that the presence of different counteranions in different stoichiometries (0.5–2 equiv) did not influence the overall conformation of the iminium cation, although some

smaller conformational adjustments are possible. Key structural features of **26** include an *s-trans* conformation adopted by the unsaturated imine moiety, with both double bonds possessing (*E*)-geometry. Analysis of  $^{15}\text{N}$  chemical shifts and  $^1J_{\text{H-N}}$  coupling constants in monoprotonated salts **26a** and **26c** revealed full protonation of the quinuclidine nitrogen and partial protonation of the imine nitrogen, consistent with an internal hydrogen bond forming a pseudofive-membered ring  $\text{N}_1\text{-C}_8\text{-C}_9\text{-N}_{21}\text{-H}$  (Figure 2). In the presence of 2 equiv of a Brønsted acid (salts **26b** and **26d**), this hydrogen bond was found to be undisturbed, with the second site of protonation being the quinoline nitrogen.<sup>17</sup> The effect of this internal hydrogen bonding manifests itself in the hindrance of  $\text{C}_9\text{-N}_{21}$  bond rotation and  $\text{C}_8\text{-C}_9$  bond rotation (with  $\text{H}_8$  and  $\text{H}_9$  adopting an *anti* relationship). Indeed, the only dynamic moiety was found to be the quinoline group, which undergoes rapid conformational exchange (rotation around the  $\text{C}_9\text{-C}_4'$  bond) at room temperature in unprotonated imine **25** and a somewhat hindered rotation in the protonated iminium species **26** as witnessed by corresponding peak broadening and NOESY analysis.<sup>17</sup>

Although diffusion ordered spectroscopy (DOSY) indicated a tight association of the ammonium cation and the counteranion in salts **26** in aprotic or weakly protic media,<sup>17</sup> heteronuclear NOE experiments failed to pinpoint the position of the counteranion in solution. In both TFA and (*R*)-TRIP salts, a large number of weak cross-peaks from the  $^{19}\text{F}$  or  $^{31}\text{P}$  nucleus to  $^1\text{H}$  signals from all three subcomponents of **25** (quinuclidine, quinoline, and aza-diene) with similar intensities was observed, suggesting some flexibility in the ion pairing.<sup>54</sup>

Nevertheless, the strong influence of the Brønsted acid cocatalyst on the enantioselectivity of our epoxidation reactions suggested involvement of the counteranion in the asymmetric induction. In order to probe this hypothesis further, we examined the effect of ion separation by a protic solvent. To this end, we carried out the epoxidation of enal **19a** in methanol, which was confirmed by DOSY analysis to completely separate the ammonium cation and the counteranion in salt **26c** without affecting the overall conformation of the protonated imine.<sup>17</sup>

As demonstrated in Table 12, carrying out the epoxidation in methanol resulted in complete erosion of the reaction's

**Table 12. The Effect of an Ion-Separating Solvent on the Epoxidation of 19a with Catalytic Ammonium Salts of 1a**

entry	acid	solvent	conv. [%] <sup>a</sup>	dr <sup>a</sup>	er ( <i>trans</i> ) <sup>b</sup>
1	( <i>R</i> )- <b>21a</b>	MeOH	37 <sup>c</sup>	51:49	43:57
2	TFA	MeOH	78	51:49	46:54
3	( <i>R</i> )- <b>21a</b>	THF	81	87:13	99:1
4	TFA	THF	73	65:35	75:25

<sup>a</sup>Determined by GC. <sup>b</sup>Determined by GC with a chiral stationary phase. <sup>c</sup>The catalyst salt was poorly soluble.

diastereoselectivity and a greatly reduced and reversed enantioselectivity (compare entries 1–2 to entries 3–4), although the conversion remained high (the lower conversion obtained with the salt [**1a**-(*R*)-**21a**] in methanol reflects poor catalyst solubility). More importantly, very similar results were

obtained with either chiral or achiral acid cocatalyst in methanol (entries 1–2). These findings suggest that while an acid additive can catalyze the reaction even in a disruptive protic solvent by protonating the imine intermediate of type **25**, it has no influence on the stereoselectivity of the reaction if the ions are solvent separated.<sup>55</sup>

In a parallel line of investigations, we performed the epoxidation of enal **19a** in a nondisruptive aprotic solvent but employed Brønsted acid cocatalysts whose conjugate bases form anions of different coordinating strengths. Figure 3 shows

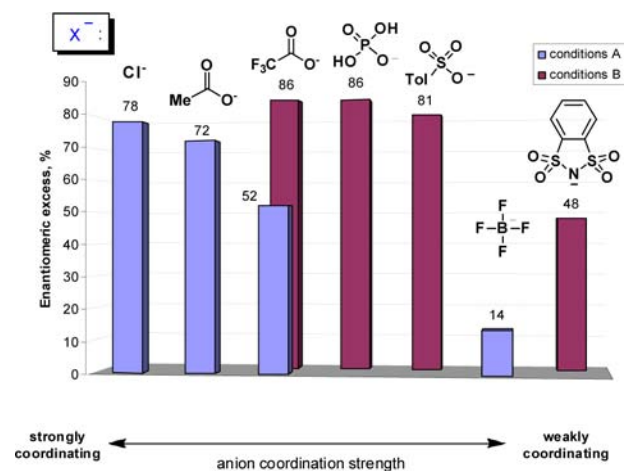


**Figure 3.** The effect of the counteranion coordination strength in catalyst salts [**1a**-2HX] on the enantioselectivity of enal epoxidation. Conditions A: THF, 50%  $\text{H}_2\text{O}_2$  (5 equiv) and B: 1,4-dioxane, 50%  $\text{H}_2\text{O}_2$  (1.5 equiv).

the enantiomeric excess of the major *trans*-diastereomer **20a** obtained with each of the counteranions  $\text{X}^-$  in the catalytic salts [**1a**-2HX] (see Supporting Information for conversion and dr). Approximate relative coordinating strength of the screened counteranions is provided along the *x*-axis.<sup>56</sup> A clear trend can be observed with respect to counteranion association in the catalytic salt [**1a**-2HX] and the enantioselectivity of the reaction. In particular, the most tightly coordinating anions gave the highest enantiomeric excess, even without possessing chirality themselves.

**Computational Studies and the Proposed Model of Stereoselectivity.** With the structure of the ammonium cation established by physical methods and evidence for the involvement of the counteranion in the asymmetric induction, we turned to computation to complete the model of stereoselectivity. Toward this end, we analyzed the geometries of TSs for the enantiodetermining step, i.e., hydrogen peroxide attack on the iminium ion. We employed DFT throughout. Geometry optimizations were performed using the BP86 functional and the def2-SVP basis set. Single-point calculations at the BP86/def2-SVP optimized geometries were carried out with larger basis sets (def2-TZVP) and different functionals (B3LYP, M06, M06-2X) and with inclusion of continuum solvation and empirical dispersion corrections to arrive at more accurate energetics. Thermal and entropic corrections were evaluated at the BP86/def2-SVP level to convert the calculated energies into free energies. The Supporting Information contains detailed information on the applied computational methods and the numerical results as well as more detailed discussions of the results obtained for the various pathways considered. In the following, we focus on the two major

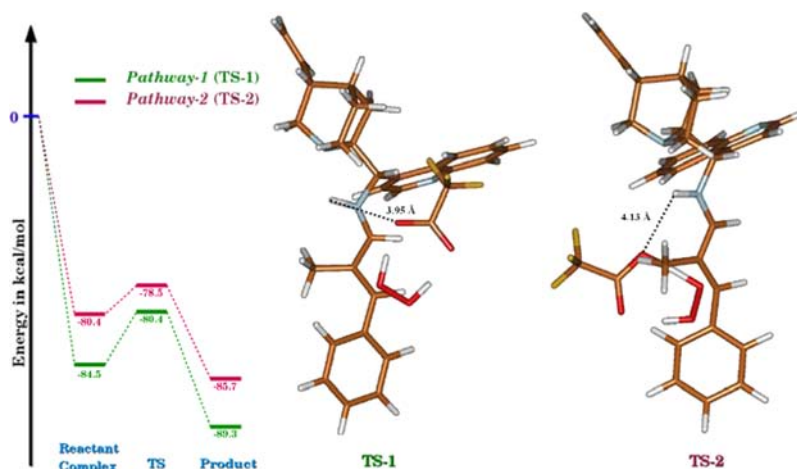


**Figure 4.** Energetically lowest-lying reaction pathways and TS leading to the favored enantiomer (pathway 1, left structure) and the unfavored enantiomer (pathway 2, right structure) computed at the BP86/def2-SVP level. See Table 3, Supporting Information, for further information.

pathways. The quoted free energy differences are either taken directly from the BP86/def2-SVP results or represent best estimates derived from single-point B3LYP/def2-TZVP data with all aforementioned corrections included.

Preliminary calculations revealed that the counteranion and hydrogen peroxide generally approach the iminium ion from the same side, allowing the anion to take up the proton liberated during this reaction step. We chose to use the iminium ion derived from 9-amino(9-deoxy)epicinchonidine **1d**, which corresponds to **1a** with an unsubstituted quinoline group, and enal **19e**, together with TFA, as our model system (Figure 4).<sup>57</sup>

We considered four different pathways in the TS modeling: the quinoline group can adopt two different orientations (up and down) during the approach of the anion and hydrogen peroxide from the ( $\beta$ )-*si*-face or ( $\beta$ )-*re*-face, giving rise to TSs **TS-1** and **TS-3** (*si*) or **TS-2** and **TS-4** (*re*). For each of these pathways, a series of starting geometries were screened at the BP86/def2-SVP level to locate the lowest-energy TS for hydrogen peroxide attack.<sup>58</sup>

For the peroxide approach from the ( $\beta$ )-*si*-face, the orientation of the quinoline group has little influence on the energetics, since the conformer with this group pointing toward the anion (**TS-1**, Figure 4) is only slightly favored (by 0.8 kcal/mol, BP86) over the alternative one (**TS-3**) due to C–H...F hydrogen-bonding interactions with TFA (2.43–2.58 Å). The lowest-energy TS for peroxide attack from the ( $\beta$ )-*re*-face (**TS-2**) also has the quinoline group pointing toward the anion, with the alternative orientation (**TS-4**) being rather strongly disfavored (by 4.3 kcal/mol, BP86). Importantly, both TSs for the ( $\beta$ )-*si*-face attack are lower in energy than those for ( $\beta$ )-*re*-face attack. The relevant free energy difference between **TS-1** and **TS-2** amounts to 1.9 kcal/mol (BP86) or 2.4 kcal/mol (best B3LYP-based estimate).

Several common features can be noted when comparing the two lowest-lying TSs that lead to the major and minor enantiomer, respectively (**TS-1** and **TS-2**). In both cases, the peroxide O–H bond is broken, and the C–O bond is formed in a concerted way, resulting in a direct proton transfer to the counteranion. The second O–H bond of the nonattacking peroxide oxygen is also coordinated to the counteranion. Another common feature is the formation of a pseudofive-membered ring N<sub>1</sub>–C<sub>8</sub>–C<sub>9</sub>–H<sub>21</sub>–H, as already seen in the

NMR structure of **26** (Figure 2). This coordination also implies that the quinuclidine nitrogen is not directly involved in directing the peroxide attack.

There are also considerable differences between **TS-1** and **TS-2**, which are helpful in rationalizing the observed enantioselectivity. In **TS-1** the configuration around the newly formed C–O bond is almost perfectly staggered, the anion being roughly oriented toward the positively charged iminium ion. The distance between the closer TFA oxygen and the iminium proton is 3.95 Å. On the other hand, for **TS-2**, in order to avoid a steric clash with the quinoline moiety, the TFA-peroxide adduct prefers a different orientation. Here, the configuration around the C–O bond is close to eclipsed, and the cation anion distance is increased to 4.13 Å. As the anion is much better accommodated on one side of the iminium ion and directs hydrogen peroxide to the same side, it effectively acts as a mediator, communicating the steric information around the catalysts stereocenter to the rather distant point of attack.

Our model predicts that the quinoline moiety should influence enantioselection, but a degree of conformational flexibility is allowed, as the two most stable rotamers around the C<sub>9</sub>–C<sub>4</sub> bond both favor the same enantiomer. As described previously, such flexibility of the quinoline ring in imine salts **26** was indeed observed by NMR experiments. Furthermore, experiments using the truncated catalyst, which lacks a quinoline moiety, revealed that this group is indeed essential for the stereoselection.<sup>17</sup>

Based on our model of stereoselectivity, we propose that the excellent catalytic efficiency of the *N*-oxidized amine **24** stems from its ability to form structurally similar iminium salts **27**, which participate in the enantiodetermining C–O bond-forming event (Figure 5). In particular, our data suggest that the *N*-oxide moiety simply expands the internal hydrogen-bonded assembly observed in salts **26** by one oxygen atom, forming a pseudosix-membered ring and thus causing little perturbation in the TS. A similar type of intramolecular hydrogen bonding has been reported in chiral *N,N*-dioxide amide catalysts.<sup>59</sup>

In order to generalize our enantioselectivity model to the epoxidation of enone substrates, and indeed any Michael reaction of unsaturated carbonyl compounds catalyzed by **1a**, structural information about the iminium intermediate of type



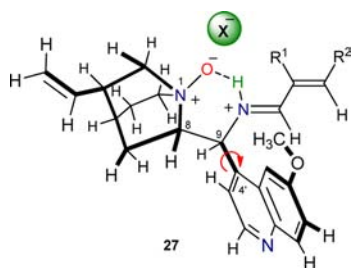


**Figure 5.** Proposed structure of monoprotonated iminium **27** derived from the N-oxidized catalyst **24**.

A (Scheme 8) is required. In particular, with all other parameters being equal, the imine C=N bond geometry is expected to determine the absolute facial selectivity of the Michael addition. Unfortunately, attempts to synthesize imine intermediates from enones for conformational studies did not meet with success. However, computational studies by Chen and colleagues on the epoxidation of 2-cyclohexen-1-one **9a** by chiral cinchona alkaloid-derived amine salts<sup>58</sup> and those of Zhu, Liu, and co-workers on the epoxidation of the same substrate by a chiral primary diamine salt<sup>60</sup> both suggest iminium intermediates with the Z-configured C=N bond as the catalytically relevant species leading to the epoxide product. These results are in agreement with our stereochemical model, which correctly predicts the experimentally observed absolute configuration for all enone substrate classes (cyclic, acyclic, and macrocyclic), as long as the iminium intermediates are Z-configured (Figure 6).

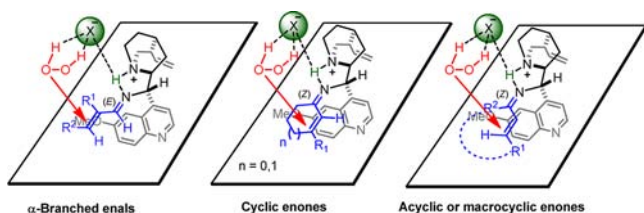


**Figure 6.** Stereoselectivity Mnemonic for Epoxidation Reactions of Unsaturated Carbonyl Compounds Catalyzed by Amine **1a**.

While we do not yet have experimental proof for this mechanism of stereoselectivity with the enone substrates, the models depicted in Figure 6 can serve as a useful guide for predicting enantioselectivity. Indeed, we expect this mnemonic to be applicable to any Michael addition of protic nucleophiles to unsaturated carbonyl compounds catalyzed by **1a** and its closely related derivatives, given the remarkable consistency in the stereochemical outcome reported in the literature.

## CONCLUSIONS

We have demonstrated that the readily available cinchona alkaloid-derived primary amines **1** serve as powerful catalysts in the asymmetric epoxidation and peroxidation of various carbonyl compounds with hydrogen peroxide. The reactions have been shown to tolerate a wide scope of aliphatic acyclic  $\alpha,\beta$ -unsaturated ketones, small, medium and large ring-sized cyclic  $\alpha,\beta$ -unsaturated ketones, and  $\alpha$ -branched  $\alpha,\beta$ -unsaturated aldehydes, giving rise to an enantiomeric excess of generally above 95:5 er. Stereoconvergence with respect to the substrate double-bond geometry and significant catalyst control over pre-existing stereogenic centers is a feature of most of the presented

epoxidations. In addition to providing direct access to optically active peroxide and epoxide products, the described methods allow for further product functionalization to generate such useful building blocks as  $\beta$ -hydroxyketones, 1,2-dioxolanes, and epoxyalcohols without any erosion of the enantiomeric excess. Detailed mechanistic investigations provide extensive support for covalent aminocatalysis and shed light on an unusual nondetrimental catalyst oxidation pathway. In addition, NMR and computational studies allowed for the rationalization of the origin of stereoselectivity induced by the ammonium salts of **1**. Importantly, we have elucidated the role of the counteranion provided by the Brønsted acid cocatalyst, which translates remote chirality of the ammonium cation to the reaction center and functions as a base to activate the nucleophile. Given the excellent enantioselectivity and substrate scope, we anticipate utility of our methods in synthesis.

## ASSOCIATED CONTENT

### Supporting Information

Experimental part: procedures, compound characterization, NMR spectra, and GC and HPLC traces for all new compounds. Computational part: methods, detailed numerical results for energies, optimized Cartesian coordinates, and further discussion of the computational results. This material is available free of charge via the Internet at <http://pubs.acs.org>.

## AUTHOR INFORMATION

### Corresponding Author

[list@kofo.mpg.de](mailto:list@kofo.mpg.de)

### Notes

The authors declare no competing financial interest.

## ACKNOWLEDGMENTS

This study has been generously supported by the Deutsche Forschungsgemeinschaft (DFG), the Max-Planck-Gesellschaft (MPG), and the Fonds der Chemischen Industrie (FCI). We thank our GC, HPLC, mass spectrometry, and NMR departments as well as Marianne Hannappel, Simone Marcus, Petra Philipps, Natascha Wippich for technical assistance.

## REFERENCES

- (1) Sharpless, K. B. *Angew. Chem., Int. Ed.* **2002**, *41*, 2024.
- (2) (a) Wynberg, H.; Greijdanus, B. *J. Chem. Soc. Chem. Commun.* **1978**, 427. (b) Juila, S.; Guixer, J.; Masana, J.; Rocas, J.; Colonna, S.; Annuziata, R.; Molinari, H. *J. Chem. Soc. Perkin Trans. 1* **1982**, 1317. (c) Katsuki, T.; Sharpless, K. B. *J. Am. Chem. Soc.* **1980**, *102*, 5976. (d) Irie, R.; Noda, K.; Ito, Y.; Matsumoto, N.; Katsuki, T. *Tetrahedron Lett.* **1990**, *31*, 7345. (e) Zhang, W.; Loebach, J. L.; Wilson, S. R.; Jacobsen, E. N. *J. Am. Chem. Soc.* **1990**, *112*, 2801. (f) Enders, D.; Zhu, J.; Raabe, G. *Angew. Chem., Int. Ed. Engl.* **1996**, *35*, 1725. (g) Yang, D.; Yip, Y.-C.; Tang, M.-W.; Wong, M.-K.; Zheng, J.-H.; Cheung, K.-K. *J. Am. Chem. Soc.* **1996**, *118*, 491. (h) Bougauchi, M.; Watanabe, S.; Arai, T.; Sasai, H.; Shibasaki, M. *J. Am. Chem. Soc.* **1997**, *119*, 2329. (i) Wang, Z.-X.; Tu, Y.; Frohn, M.; Zhang, J.-R.; Shi, Y. *J. Am. Chem. Soc.* **1997**, *119*, 11224. (j) Watanabe, S.; Arai, T.; Sasai, H.; Bougauchi, M.; Shibasaki, M. *J. Org. Chem.* **1998**, *63*. (k) Corey, E. J.; Zhang, F.-Y. *Org. Lett.* **1999**, *1*, 1287. (l) Jacques, O.; Richards, S. J.; Jackson, R. F. *W. Chem. Commun.* **2001**, 2712. (m) Li, C.; Pace, E. A.; Liang, M. C.; Lobkovsky, E.; Gilmore, T. D.; Porco, J. A., Jr. *J. Am. Chem. Soc.* **2001**, *123*, 11308. (n) Berkessel, A.; Guixa, M.; Schmidt, F.; Neudörfl, J. M.; Lex, J. *Chem.—Eur. J.* **2007**, *13*, 4483. (o) Erkkilä, A.; Pihko, P. M.; Clarke, M.-R. *Adv. Synth. Catal.* **2007**, *349*, 802. (p) Peris, G.; Jakobsche, C. E.; Miller, S. J. *J. Am. Chem. Soc.* **2007**, *129*, 8710. (q) Zhang, W.; Yamamoto, H. *J. Am. Chem. Soc.* **2007**, *129*, 286. For

reviews, see: (r) Porter, M. J.; Skidmore, J. *Chem. Commun.* **2000**, 1215. (s) Adam, W.; Saha-Möllner, C. R.; Ganeshpure, P. A. *Chem. Rev.* **2001**, *101*, 3499. (t) Lane, B. S.; Burgess, K. *Chem. Rev.* **2003**, *103*, 2457. (u) Xia, Q.-H.; Ge, H.-Q.; Ye, C.-P.; Liu, Z.-M.; Su, K.-X. *Chem. Rev.* **2005**, *105*, 1603. (v) Lattanzi, A. *Curr. Org. Synth.* **2008**, *5*, 117.

(3) Weitz, E.; Scheffer, A. *Chem. Ber.* **1921**, *54*, 2344.

(4) (a) Bunton, C. A.; Minkoff, G. J. *J. Chem. Soc.* **1949**, 665. (b) Christian, C. F.; Takeya, T.; Szymanski, M. J.; Singleton, D. A. *J. Org. Chem.* **2007**, *72*, 6183. (c) House, H. O.; Ro, R. S. *J. Am. Chem. Soc.* **1958**, *80*, 2428. (d) Kelly, D. R.; Caroff, E.; Flood, R. W.; Heal, W.; Roberts, S. M. *Chem. Commun.* **2004**, 2016. (e) Kelly, D. R.; Roberts, S. M. *Pept. Sci.* **2006**, *84*, 74. (f) Meerwein, H. *J. Prakt. Chem.* **1926**, *113*, 9. (g) Weitz, E.; Scheffer, A. *Chem. Ber.* **1921**, *54*, 2344. (h) Wright, P.; Abbot, J. *Int. J. Chem. Kinet.* **1993**, *25*, 901. It was later shown that for metallated peroxides, the reaction sometimes proceeds through a concerted asynchronous manner. For a discussion, see: (i) Švenda, J.; Myers, A. G. *Org. Lett.* **2009**, *11*, 2437. However we are not aware of any such observation for the organocatalytic variant of the reaction.

(5) (a) Marigo, M.; Franzen, J.; Poulsen, T. B.; Zhuang, W.; Jørgensen, K. A. *J. Am. Chem. Soc.* **2005**, *127*, 6964–6965. (b) Sundén, H.; Ibrahim, L.; Cordova, A. *Tetrahedron Lett.* **2006**, *47*, 99. (c) Lee, S.; MacMillan, D. W. C. *Tetrahedron* **2006**, *62*, 11413.

(6) (a) Wang, X.; List, B. *Angew. Chem., Int. Ed.* **2008**, *47*, 1119. For reviews on ACDC, see: (b) Mahlau, M.; List, B. *Angew. Chem., Int. Ed.* **2013**, *52*, 518. (c) Phipps, R. J.; Hamilton, G. L.; Toste, F. D. *Nat. Chem.* **2012**, *4*, 603. (d) Mahlau, M.; List, B. *Isr. J. Chem.* **2012**, *52*, 630. (e) Ratjen, L.; Müller, S.; List, B. *Nachr. Chem.* **2010**, *58*, 640.

(7) For a single example of secondary amine catalysis used in the epoxidation of  $\alpha$ -branched acroleins, see: (a) Bondzic, B. P.; Urushima, T.; Ishikawa, H.; Hayashi, Y. *Org. Lett.* **2010**, *12*, 5434. For examples using noncovalent organocatalysis for Weitz–Scheffer-type epoxidation, see: (b) Lattanzi, A. *Org. Lett.* **2005**, *7*, 2579. (c) Russo, A.; Galdi, G.; Croce, G.; Lattanzi, A. *Chem.—Eur. J.* **2012**, *18*, 6152.

(8) (a) Martin, N. J. A.; List, B. *J. Am. Chem. Soc.* **2006**, *128*, 13368. (b) Reisinger, C. M.; Wang, X.; List, B. *Angew. Chem., Int. Ed.* **2008**, *47*, 8112. (c) Wang, X.; Reisinger, C. M.; List, B. *J. Am. Chem. Soc.* **2008**, *130*, 6070. (d) Zhou, J.; Wakchaure, V.; Kraft, P.; List, B. *Angew. Chem., Int. Ed.* **2008**, *47*, 7656. (e) Lifchits, O.; Reisinger, C. M.; List, B. *J. Am. Chem. Soc.* **2010**, *132*, 10227. (f) Jiang, G.; List, B. *Angew. Chem., Int. Ed.* **2011**, *50*, 9471. (g) Lee, A.; Michrowska, A.; Sulzer-Mosse, S.; List, B. *Angew. Chem., Int. Ed.* **2011**, *50*, 1707. (h) Lee, A.; List, B. *Adv. Synth. Catal.* **2012**, *354*, 1701.

(9) (a) Ishihara, K.; Nakano, K. *J. Am. Chem. Soc.* **2005**, *127*, 10504. (b) Huang, H.; Jacobsen, E. N. *J. Am. Chem. Soc.* **2006**, *128*, 7170. (c) Lalonde, M. P.; Chen, Y.; Jacobsen, E. N. *Angew. Chem., Int. Ed.* **2006**, *45*, 6366–6370. (d) Kim, H.; Yen, C.; Preston, P.; Chin, J. *Org. Lett.* **2006**, *8*, 5239. (e) Ishihara, K.; Nakano, K. *J. Am. Chem. Soc.* **2007**, *129*, 8930. (f) Xie, J.-W.; Chen, W.; Li, R.; Zeng, M.; Du, W.; Yue, L.; Chen, Y.-C.; Wu, Y.; Zhu, J.; Deng, J.-G. *Angew. Chem., Int. Ed.* **2007**, *46*, 389.

(10) (a) Peng, F.; Shao, Z. *J. Mol. Catal. A: Chem.* **2008**, *285*, 1. (b) Xu, L. W.; Luo, J.; Lu, Y. *Chem. Commun.* **2009**, 1807. (c) Xu, L.-W.; Lu, Y. *Org. Biomol. Chem.* **2008**, *6*, 2047.

(11) (a) Chen, Y.-C. *Synlett* **2008**, 13, 1919. (b) Jiang, L.; Chen, Y.-C. *Catal. Sci. Technol.* **2011**, *1*, 354. (c) Yeboah, E. M. O.; Yeboah, S. O.; Singh, G. S. *Tetrahedron* **2011**, *67*, 1725. (d) Li, J.-L.; Fu, N.; Zhang, L.; Zhou, P.; Luo, S.; Cheng, J.-P. *Eur. J. Org. Chem.* **2010**, *35*, 6840. (e) Lu, X.; Liu, Y.; Sun, B.; Cindric, B.; Deng, L. *J. Am. Chem. Soc.* **2008**, *130*, 8134. (f) Lu, Y.; Zheng, C.; Yang, Y.; Zhao, G.; Zou, G. *Adv. Synth. Catal.* **2011**, *353*, 3129. (g) Melchiorre, P. *Angew. Chem., Int. Ed.* **2012**, *51*, 9748.

(12) For the original report describing preparation of **1a**, see: Brunner, H.; Bügler, J.; Nuber, B. *Tetrahedron: Asym.* **1995**, *6*, 1699.

(13) Organocatalytic methodologies for the peroxidation and epoxidation of aliphatic enones have appeared since; see refs 11e and 11f.

(14) (a) Bentley, P. A.; Bergeron, S.; Cappi, M. W.; Hibbs, D. E.; Hursthouse, M. B.; Nugent, T. C.; Pulido, R.; Roberts, S. M.; Wu, L. E. *Chem. Commun.* **1997**, 739. (b) Daikai, K.; Hayano, T.; Kino, R.; Furuno, H.; Kagawa, T.; Inanaga, J. *Chirality* **2003**, *15*, 83. (c) Ooi, T.; Ohara, D.; Tamura, M.; Maruoka, K. *J. Am. Chem. Soc.* **2004**, *126*, 6844.

(15) (a) Cativiela, C.; Figueras, F.; Fraile, J. M.; García, J. I.; Mayoral, J. A. *Tetrahedron Lett.* **1995**, *36*, 4125. (b) Fraile, J. M.; García, J. I.; Mayoral, J. A.; Sebtí, S.; Tahirb, R. *Green Chem.* **2001**, *3*, 271. (c) Payne, G. J. *Org. Chem.* **1958**, *23*, 310. (d) Rieche, A.; Schmitz, E.; Gründemann, E. *Chem. Ber.* **1960**, *93*, 2443.

(16) (a) Barnier, J.-P.; Morisson, V.; Blanco, L. *Synth. Commun.* **2001**, *31*, 349. (b) Kulinkovich, O. G.; Astashko, D. A.; Tyvorskii, V. I.; Ilyina, N. A. *Synthesis* **2001**, *10*, 1453.

(17) See Supporting Information for further details.

(18) Other hydroxy-group containing substrates were also tested. For details on these experiments, see the Supporting Information.

(19) (a) Yang, J. W.; Hechavarría Fonseca, M. T.; Vignola, N.; List, B. *Angew. Chem., Int. Ed.* **2005**, *44*, 108. (b) Ouellet, S. G.; Tuttle, J. B.; MacMillan, D. W. C. *J. Am. Chem. Soc.* **2005**, *127*, 32.

(20) For further support of the suggested mechanism from substrate isomerization and studies on  $\beta,\beta$ -disubstituted substrates, see the Supporting Information.

(21) Dakin, H. D. *Am. Chem. J.* **1909**, *42*, 477.

(22) (a) Bartoli, G.; Bosco, M.; Carlone, A.; Pesciaoli, F.; Sambri, L.; Melchiorre, P. *Org. Lett.* **2007**, *9*, 1403. (b) Xie, J.-W.; Huang, X.; Fan, L.-P.; Xu, D.-C.; Li, X.-S.; Su, H.; Wen, Y.-H. *Adv. Synth. Catal.* **2009**, *351*, 3077.

(23) Fehr, C.; Galindo, J. *Helv. Chim. Acta* **2005**, *88*, 3128.

(24) For the reduction of 3-hydroxy-1,2-dioxolanes with trivalent phosphorus compounds, see: (a) Baumstark, A. L.; Vasquez, P. C.; Chen, Y. *Heteroat. Chem.* **1993**, *4*, 175. (b) Morisson, V.; Barnier, J.-P.; Blanco, L. *Tetrahedron Lett.* **1999**, *40*, 4045.

(25) Carlone, A.; Bartoli, G.; Bosco, M.; Pesciaoli, F.; Ricci, P.; Sambri, L.; Melchiorre, P. *Eur. J. Org. Chem.* **2007**, 5492.

(26) For the synthesis of aldol-like products **6** from epoxy ketones, see the Supporting Information.

(27) (a) Dai, P.; Trullinger, T. K.; Liu, X.; Dussault, P. H. *J. Org. Chem.* **2006**, *71*, 2283. (b) Martyn, D. C.; Beletsky, G.; Cortese, J. F.; Tyndall, E.; Liu, H.; Fitzgerald, M. M.; O'Shea, T. J.; Liang, B.; Clardy, J. *Bioorg. Med. Chem. Lett.* **2009**, *19*, 5657. (c) Oh, D.-C.; Scott, J. J.; Currie, C. R.; Clardy, J. *Org. Lett.* **2009**, *11*, 633. (d) Scott, J. J.; Oh, D.-C.; Yuceer, M. C.; Klepzig, K. D.; Clardy, J.; Currie, C. R. *Science* **2008**, *322*, 63.

(28) For synthetic approaches to racemic 1,2-dioxolanes, see: (a) Dussault, P. H.; Lee, I. Q.; Lee, H.-J.; Lee, R. J.; Niu, Q. J.; Schultz, J. A.; Zope, U. R. *J. Org. Chem.* **2000**, *65*, 8407. (b) Dussault, P. H.; Lee, R. J.; Schultz, J. A.; Suh, Y. S. *Tetrahedron Lett.* **2000**, *41*, 5457. (c) Dussault, P. H.; Liu, X. *Org. Lett.* **1999**, *1*, 1391. (d) Dussault, P. H.; Trullinger, T. K.; Cho-Shultz, S. *Tetrahedron* **2000**, *56*, 9213. (e) Dussault, P. H.; Zope, U. *Tetrahedron Lett.* **1995**, *36*, 3655. (f) McCullough, K. J.; Nojimab, M. *Curr. Org. Synth.* **2001**, *5*, 601. (g) Tokuyasu, T.; Ito, T.; Masuyama, A.; Nojima, M. *Heterocycles* **2000**, *53*, 1293.

(29) Inanaga, J.; Kawanami, Y.; Yamaguchi, M. *Bull. Chem. Soc. Jpn.* **1986**, *59*, 1521.

(30) For details on this transformation, see the Supporting Information.

(31) Wynberg, H.; Marsman, B. *J. Org. Chem.* **1980**, *45*, 158.

(32) For a discussion of this isomerization reaction, see the Supporting Information.

(33) We also tested the more bulky *t*-Bu-substituted analog. For details, see the Supporting Information.

(34) Zhou, J.; Wakchaure, V.; Kraft, P.; List, B. *Angew. Chem., Int. Ed.* **2008**, *47*, 7656.

(35) (a) Bishara, A.; Rudi, A.; Goldberg, I.; Benayahu, Y.; Kashman, Y. *Tetrahedron* **2006**, *62*, 12092. (b) Shen, Y.-C.; Lin, J.-J.; Wu, Y.-R.; Chang, J.-Y.; Duh, C.-Y.; Lo, K. L. *Tetrahedron Lett.* **2006**, *47*, 6651.

(36) Carey, F. A.; Sundberg, R. J. *Advanced Organic Chemistry. Part A: Structure and Mechanisms: Structure and Mechanisms*, 5 ed.; Springer: New York, 2007.

(37) For the application of our epoxidation methodology in the synthesis of enantiomerically pure allylic alcohols, see: Jiang, H.; Holub, N.; Jørgensen, K. A. *Proc. Natl. Acad. Sci. U.S.A.* **2010**, *107*, 20630–20635.

(38) (a) Pidathala, C.; Hoang, L.; Vignola, N.; List, B. *Angew. Chem., Int. Ed.* **2003**, *42*, 2785. (b) Ghobril, C.; Sabot, C.; Mioskowski, C.; Baati, R. *Eur. J. Org. Chem.* **2008**, 4104.

(39) (a) Hanessian, S.; Pham, V. *Org. Lett.* **2000**, *2*, 2975. (b) Mitchell, C. E. T.; Brenner, S. E.; Ley, S. V. *Chem. Commun.* **2005**, 5346. (c) Perdicchia, D.; Jørgensen, K. A. *J. Org. Chem.* **2007**, *72*, 3565. (d) Wascholowski, V.; Knudsen, K. R.; Mitchell, C. E. T.; Ley, S. V. *Chem.—Eur. J.* **2008**, *14*, 6155. (e) Li, P.; Wen, S.; Yu, F.; Liu, Q.; Li, W.; Wang, Y.; Liang, X.; Ye, J. *Org. Lett.* **2009**, *11*, 753. (f) Mase, N.; Fukasawa, M.; Kitagawa, N.; Shibagaki, F.; Noshiro, N.; Takabe, K. *Synlett* **2010**, 2340. (g) Yoshida, M.; Hiram, K.; Narita, M.; Hara, S. *Symmetry* **2011**, *3*, 155.

(40) For details on the optimization, see ref 8h. It is interesting to note that while Mosher's acid proved to be the best acid additive, its stereoinformation had almost no influence on the selectivity of the reaction, with only 1% reduced ee in the mismatched case.

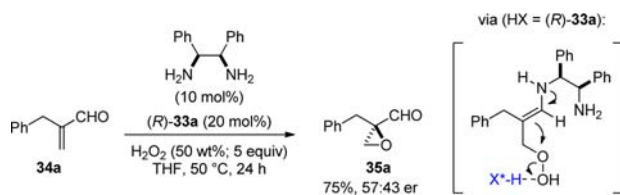
(41) (a) Payne, G. B. *J. Am. Chem. Soc.* **1959**, *81*. (b) Payne, G. B. *J. Org. Chem.* **1961**, *26*, 205. (c) Zakavi, S.; Abasi, A.; Pourali, A. R.; Rayati, S. *Bull. Korean Chem. Soc.* **2008**, *29*, 866.

(42) Organocatalytic methodologies for the epoxidation of branched acroleins have appeared since: see refs 6 and 11d.

(43) (a) Galzerano, P.; Pescioli, F.; Mazzanti, A.; Bartoli, G.; Melchiorre, P. *Angew. Chem., Int. Ed.* **2009**, *48*, 7892. (b) Ishihara, K.; Nakano, K. *J. Am. Chem. Soc.* **2007**, *129*, 8930.

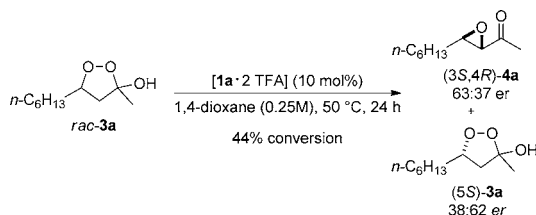
(44) Colvin, E. W.; Robertson, A. D.; Wakharkar, S. *J. Chem. Soc., Chem. Commun.* **1983**, 312.

(45) In epoxidations of  $\alpha$ -substituted acroleins **34**, where the epoxide ring closure constitutes the enantiodetermining step, employing an achiral amine with a chiral Brønsted acid cocatalyst gives enantioenriched products. See also ref 6 for similar observations with 3,3-disubstituted enals.



(46) An exception to this is the epoxidation of  $\beta,\beta$ -substituted enones **7/10** and  $\alpha$ -substituted acroleins **34**, where the initial Michael addition of hydrogen peroxide does not create a stereogenic center; it is the subsequent enamine-catalyzed ring closure that constitutes the enantiodetermining step of the reaction.

(47) We also submitted racemic peroxyhemiketal **3a** to the reaction conditions and obtained epoxide **4a** with only a low enantiomeric excess (63:37 er) resulting from a weak kinetic resolution at 44% conversion. These results are incompatible with a reversible mechanistic regime, which would be expected to furnish the epoxide **4a** with > 98.5:1.5 er via dynamic kinetic resolution, i.e. the er value observed under actual reaction conditions (see Scheme 4 and Table 2).



(48) To this goal we compared **1a** to a series of structurally distinct catalysts. For details, see the Supporting Information.

(49) (a) Arai, S.; Tsuge, H.; Shioiri, T. *Tetrahedron Lett.* **1998**, *39*, 7563. (b) Lygo, B.; Gardiner, S. D.; McLeod, M. C.; To, D. C. M. *Org. Biomol. Chem.* **2007**, *5*, 2283. (c) Lygo, B.; Wainwright, P. G. *Tetrahedron Lett.* **1998**, *39*, 1599. (d) Lygo, B.; Wainwright, P. G. *Tetrahedron* **1999**, *55*, 6289. (e) Ooi, T.; Maruoka, K. *Angew. Chem., Int. Ed.* **2007**, *46*, 4222.

(50) Oh, K.; Ryu, J. *Tetrahedron Lett.* **2008**, *49*, 1935.

(51) Lu, N.; Mi, S.; Chen, D.; Zhang, G. *Int. J. Quantum Chem.* **2011**, *111*, 2874.

(52) In contrast to the highly basic quinuclidine ( $pK_a = 11.1$  in water), tertiary amine *N*-oxides are only weakly basic ( $pK_a$  around 4.5 in water).

(53) (a) *Cinchona Alkaloids in Synthesis and Catalysis*; Song, C. E., Ed.; Wiley-VCH: Weinheim, 2009; (b) Silva, T. H. A.; Oliveira, A. B.; Santos, H. F. D.; Almeida, W. B. D. *Struc. Chem.* **2001**, *12*, 431. (c) Karle, J. M.; Karle, I. L.; Gerena, L.; Milhous, W. K. *Antimicrob. Agents Chemother.* **1992**, *36*, 1538. (d) Ferri, D.; Bürgi, T.; Baiker, A. *J. Chem. Soc. Perkin Trans. 2* **1999**, 1305. (e) Dijkstra, G. D. H.; Kellogg, R. M.; Wynberg, H.; Svendsen, J. S.; Marko, I.; Sharpless, K. B. *J. Am. Chem. Soc.* **1989**, *111*, 8069. (f) Dijkstra, G. D. H.; Kellogg, R. M.; Wynberg, H. *Recl. Trav. Chim. Pays-Bas* **1989**, *108*, 195. (g) Bürgi, T.; Baiker, A. *J. Am. Chem. Soc.* **1998**, *120*, 12920.

(54) For an example of specific ion pairing determined by heteronuclear NOESY techniques, see: (a) Olsen, R. A.; Borchardt, D.; Mink, L.; Agarwal, A.; Mueller, I. J.; Zaera, F. *J. Am. Chem. Soc.* **2006**, *128*, 15594. Hydrogen bonding interaction between the Brønsted acid and imine **41** also cannot be excluded: (b) Fleischmann, M.; Drettwan, D.; Sugiono, E.; Rueping, M.; Gschwind, R. M. *Angew. Chem.* **2011**, *123*, 6488.

(55) Similar observations were made in iminium-catalyzed intramolecular aza-Michael reaction of enones employing catalyst **1a**, where ethanol solvent also resulted in a lower and reversed enantioselectivity of the product compared to THF: Liu, J.-D.; Chen, Y.-C.; Zhang, G.-B.; Li, Z.-Q.; Chen, P.; Du, J.-Y.; Tu, Y.-Q.; Fan, C.-A. *Adv. Synth. Catal.* **2011**, *353*, 2721.

(56) (a) Díaz-Torres, R.; Alvarez, S. *Dalton Trans.* **2011**, *40*, 10742. (b) Kotlewska, A. J.; van Rantwijk, F.; Sheldon, R. A.; Arends, I. W. C. E. *Green Chem.* **2011**, *13*, 2154.

(57) Catalyst **1d** was found to give similar enantioselectivity as catalyst **1a** but has less conformational flexibility, making it ideally suited for computational purposes. Specifically, when the epoxidation of (*E*)-**31a** (eq 5) was carried out using **1d** under otherwise identical conditions, the results were close to identical. Epoxialdehyde **32a** was obtained in 44% conversion, 73:27 dr and 92:8 er (38% yield, 75:25 dr and 93:7 er with **1a**).

(58) All calculations were carried out using TURBOMOLE. See Supporting Information for computational details.

(59) Liu, X.-H.; Lin, L.-L.; Feng, X.-M. *Acc. Chem. Res.* **2011**, *44*, 574.

(60) Lv, P.-L.; Zhu, R.-X.; Zhang, D.-J.; Duan, C.-G.; Liu, C.-B. *J. Phys. Chem. A* **2012**, *116*, 1251.